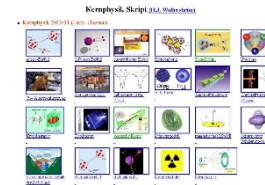


Outline: Nuclear shell structure exotic nuclei

Lecturer: Hans-Jürgen Wollersheim

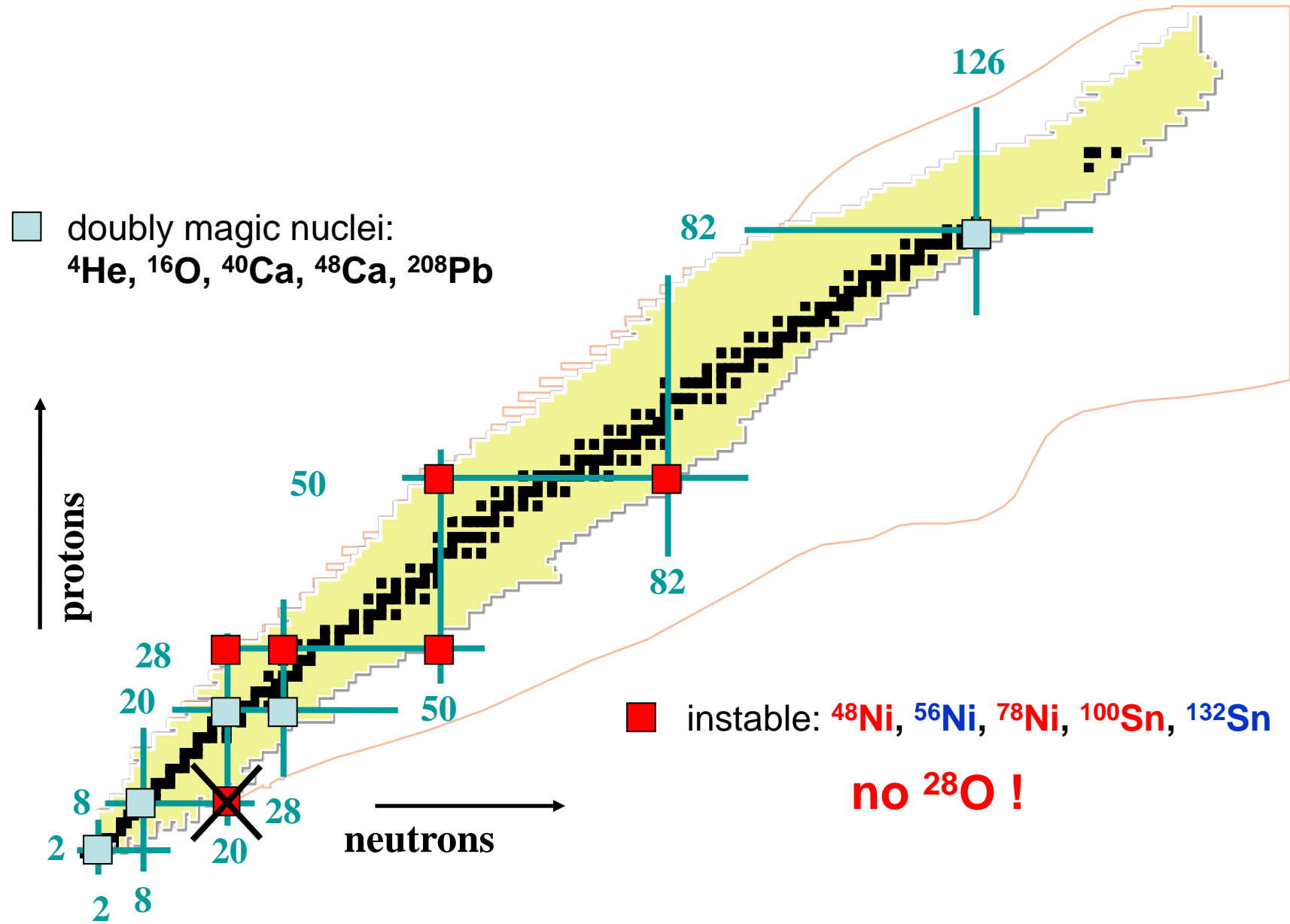
e-mail: h.j.wollersheim@gsi.de

web-page: <https://web-docs.gsi.de/~wolle/> and click on

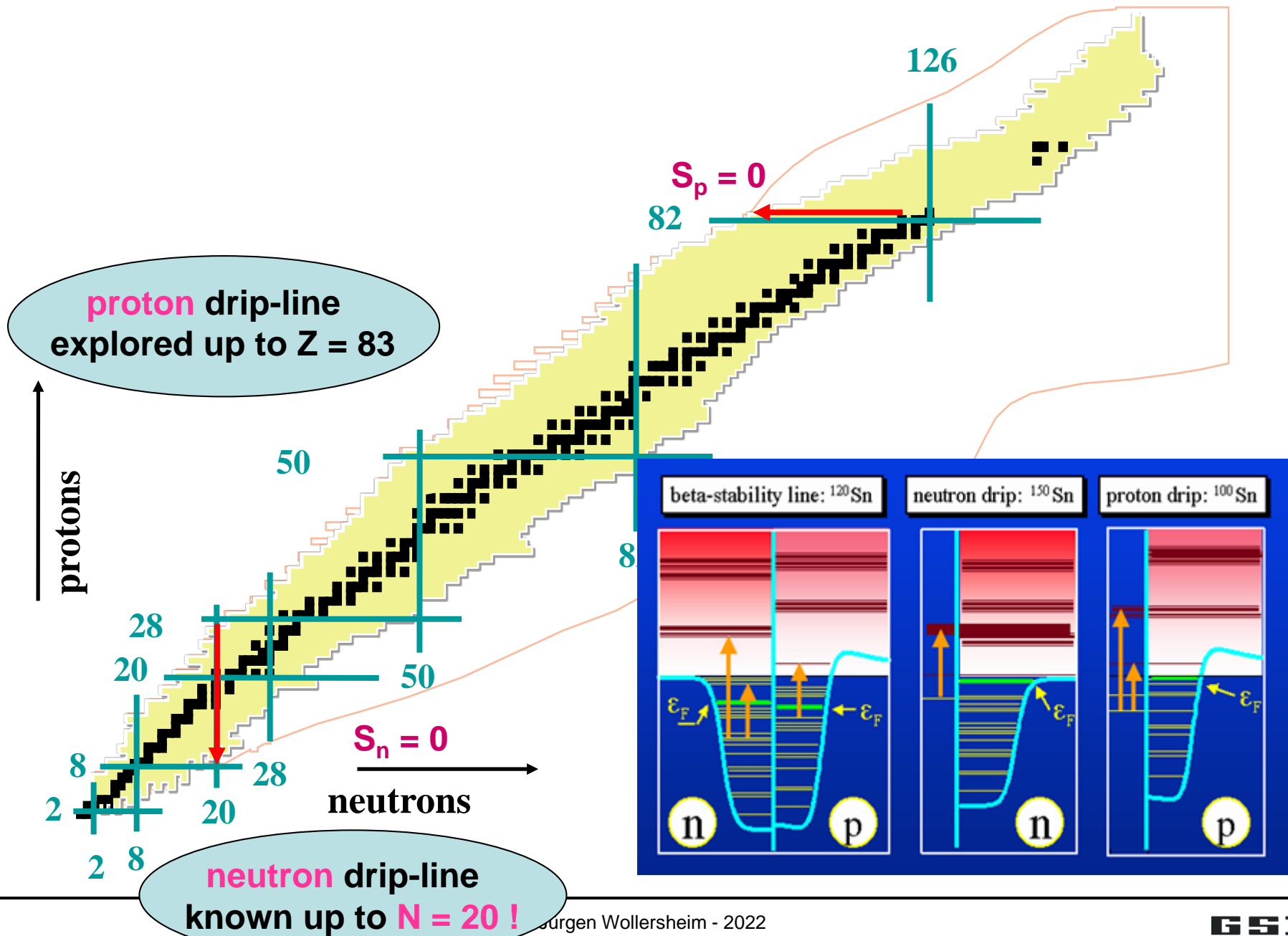


1. shell structure of super-heavy nuclei (^{250}Fm , ^{254}No)
2. classical anomalies: ^{11}Be , ^{11}Li
3. monopole interaction of the tensor force: N=20, N=28
4. neutron-proton pairing in ^{92}Pd

New challenges in nuclear structure new magic numbers

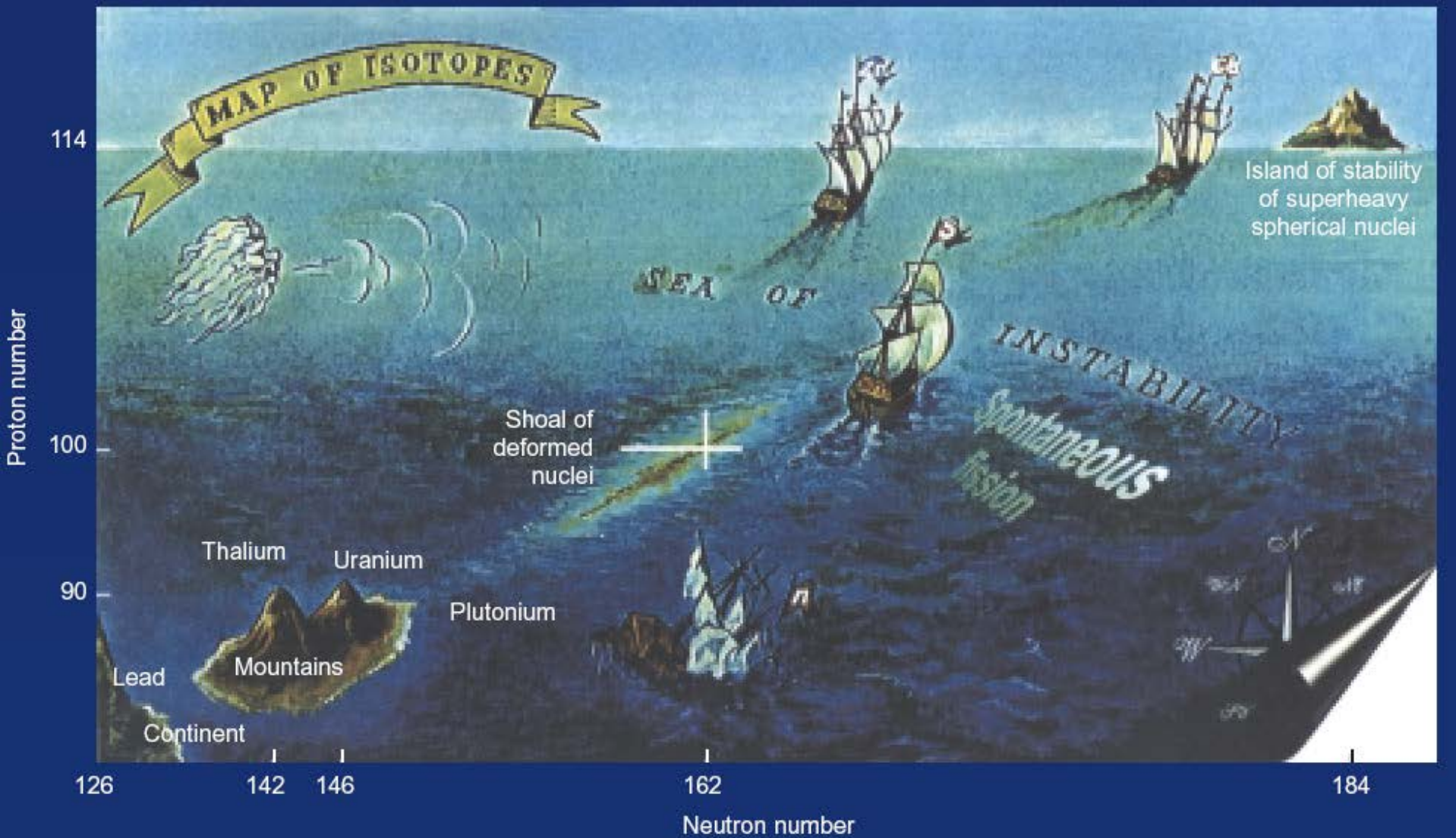


New challenges in nuclear structure new magic numbers



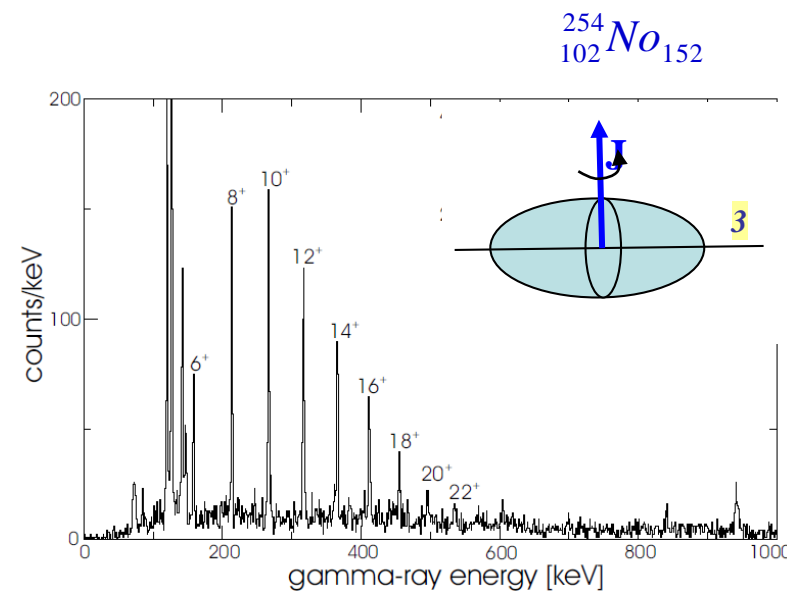
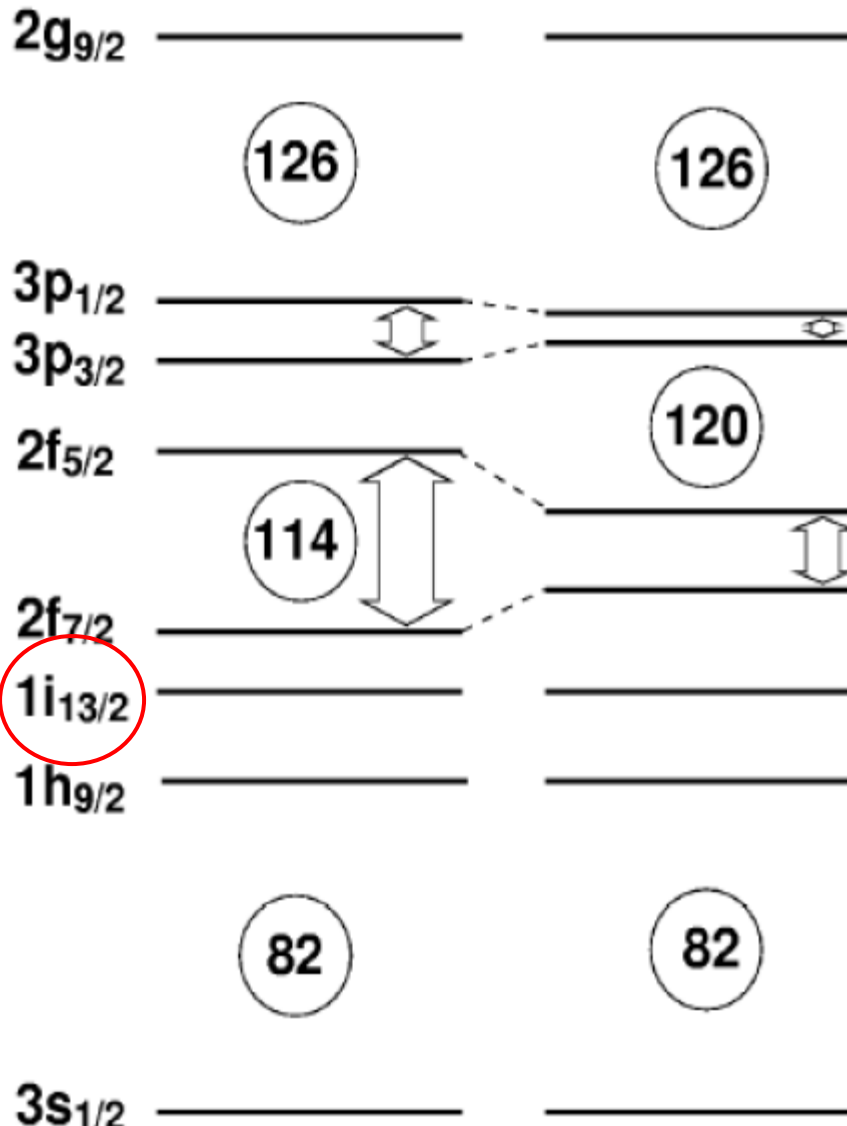
Spectroscopy of trans fermium nuclei ($Z=100-103$)

super-heavy elements

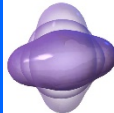


Nucleare shell structure

Where is the next shell closure ?



The **deformation** of the nucleus changes the order of the single particle states
(**Nilsson model**)



Nilsson-model

- deformed oscillator potential
- axially symmetry around the z-axis
→ nuclei can rotate

$$\omega_x = \omega_y \equiv \omega_{\perp}$$

$$\omega_x \cdot \omega_y \cdot \omega_z = \omega_0^3$$

Hamiltonian

$$H = -\frac{\hbar^2}{2 \cdot m} \cdot \Delta + \frac{m}{2} \cdot [\omega_{\perp}^2 \cdot (x^2 + y^2) + \omega_z^2 \cdot z^2] + C \cdot \vec{L} \cdot \vec{S} + D \cdot \vec{L}^2$$

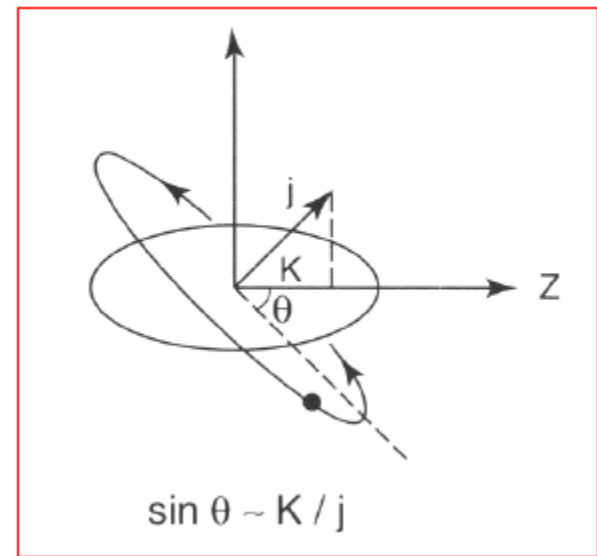
deformation parameter δ

$$\omega_{\perp}^2 = \omega_0^2 \cdot \left(1 + \frac{2}{3} \cdot \delta\right) \quad \omega_z^2 = \omega_0^2 \cdot \left(1 - \frac{4}{3} \cdot \delta\right)$$

$$H = -\frac{\hbar^2}{2 \cdot m} \cdot \Delta + \frac{m}{2} \cdot \omega_0^2 \cdot r^2 + C \cdot \vec{L} \cdot \vec{S} + D \cdot \vec{L}^2 - m \cdot \omega_0^2 \cdot r^2 \cdot \delta \cdot \frac{4}{3} \cdot \sqrt{\frac{5}{4 \cdot \pi}} \cdot Y_{20}(\theta, \phi)$$

shell model with H.O. potential

H_{def}

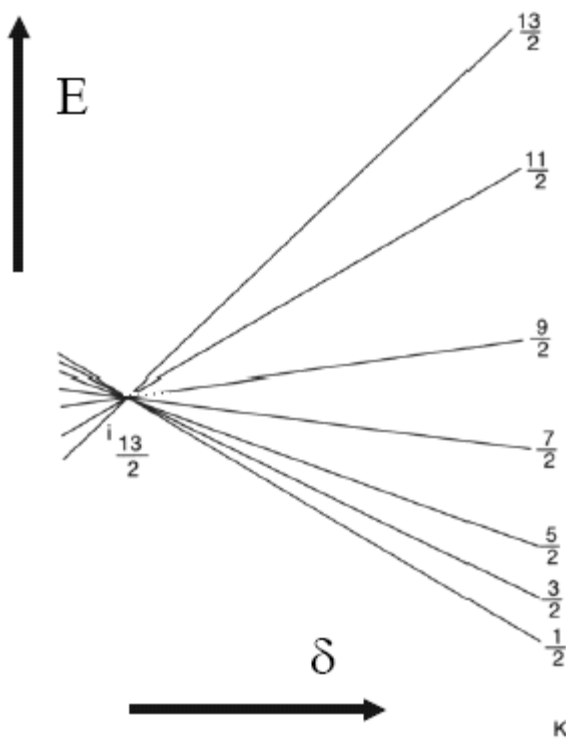


- separation of laboratory system and body-fixed (intrinsic) system
- K = projection of the single-particle angular momentum onto the symmetry axis
- Rotation perpendicular to the symmetry axis does not change the K -quantum number



Nilsson-model

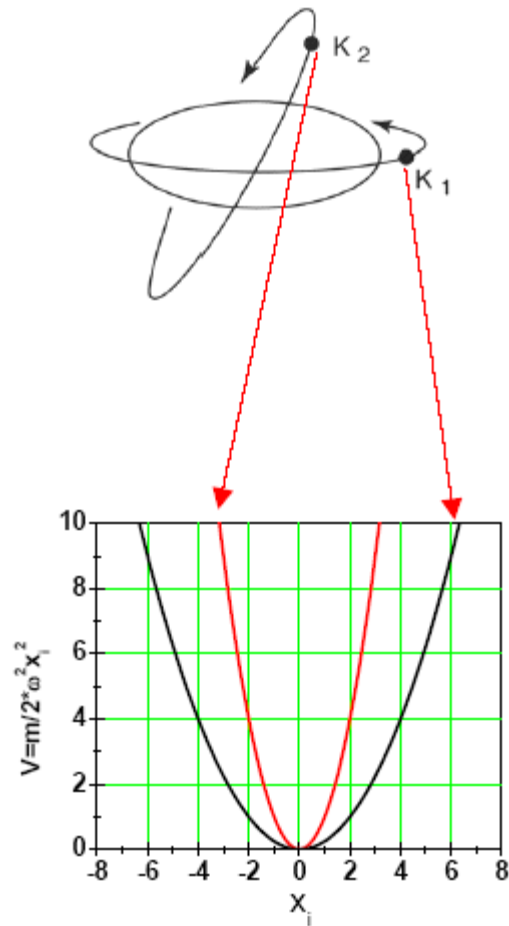
- deformed oscillator potential
- axially symmetry around the z-axis
- nuclei can rotate



Intruder

Orbitals are lifted or lowered, that orbitals from other shells with opposite parity are crossed

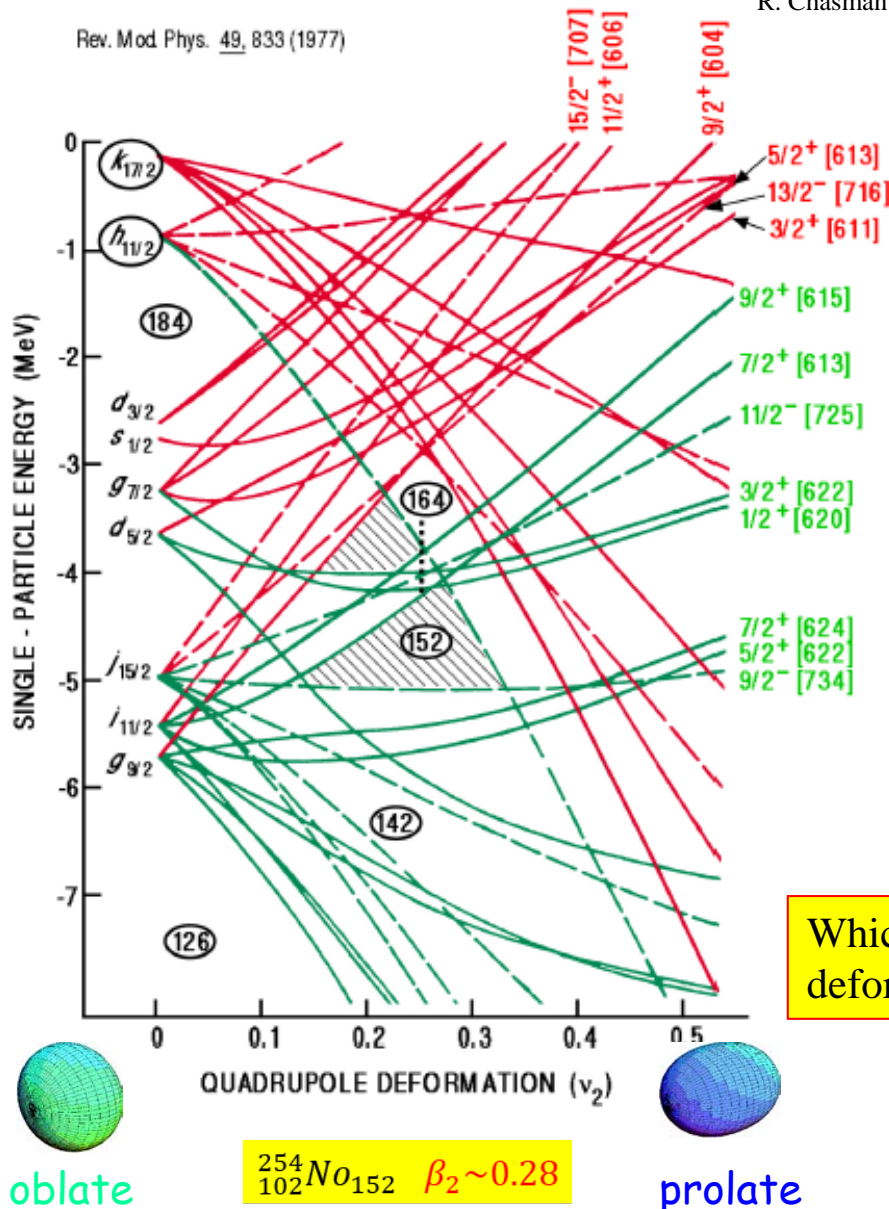
Orbital 1 is closer to the center of gravity than orbital 2.
The energy of orbital 1 is lowest.
(attention: negative sign in Hamiltonian)



Single particle orbitals

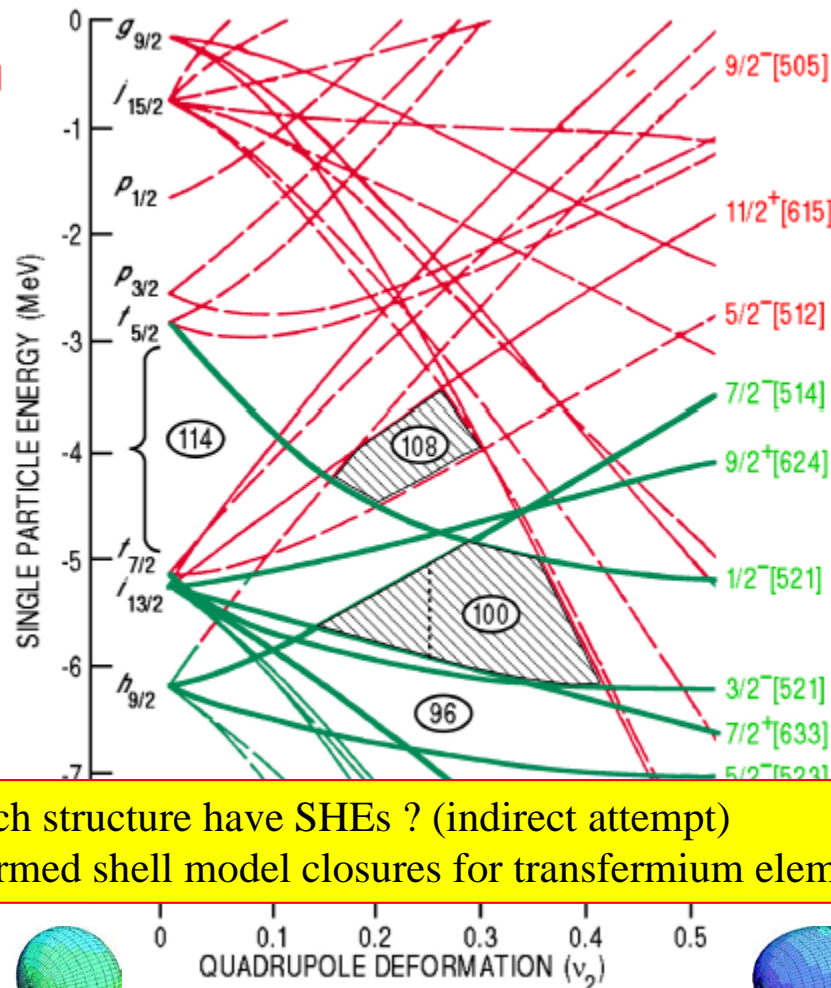
Rev. Mod. Phys. 49, 833 (1977)

R. Chasman et al. Rev. Mod. Phys. 49 (1977), 833



Rev. Mod. Phys. 49, 833 (1977)

ANL-P-22,033



Which structure have SHEs ? (indirect attempt)
deformed shell model closures for trans fermium elements

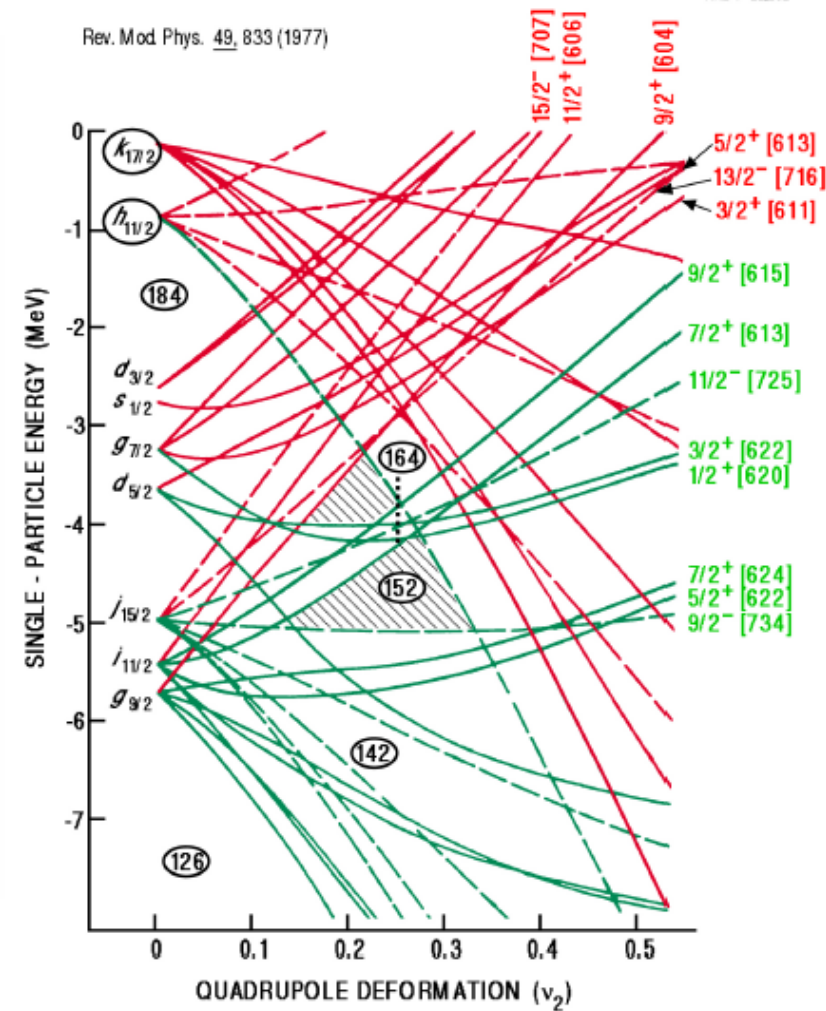
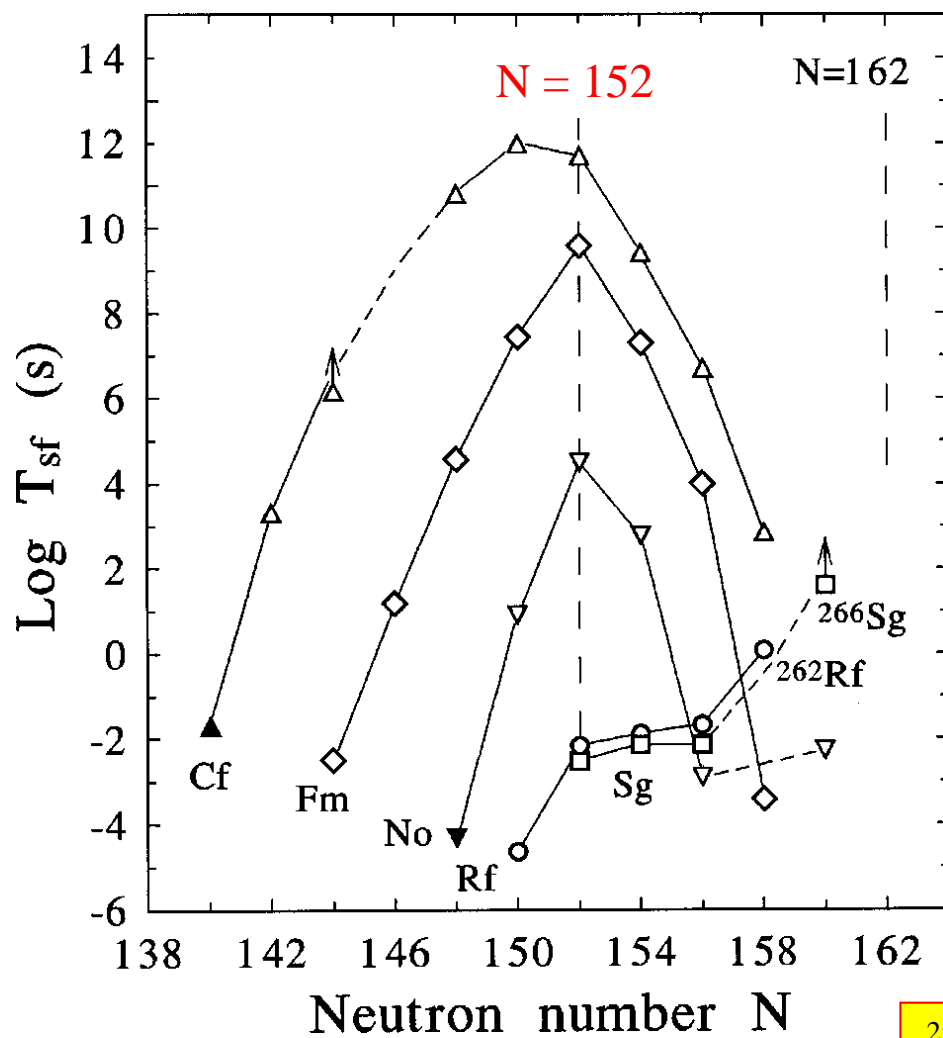
oblate

$^{254}_{102}No_{152}$ $\beta_2 \sim 0.28$

prolate

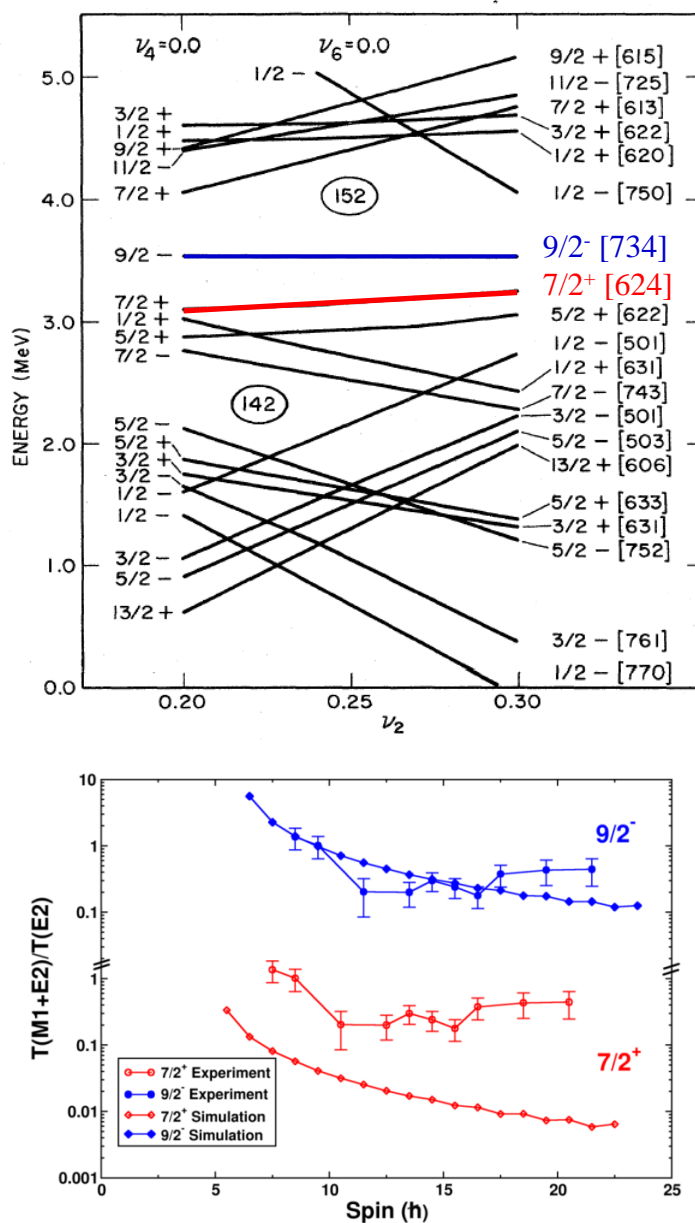
Stability of heavy elements – Nilsson energy levels

ANL-P-22.262

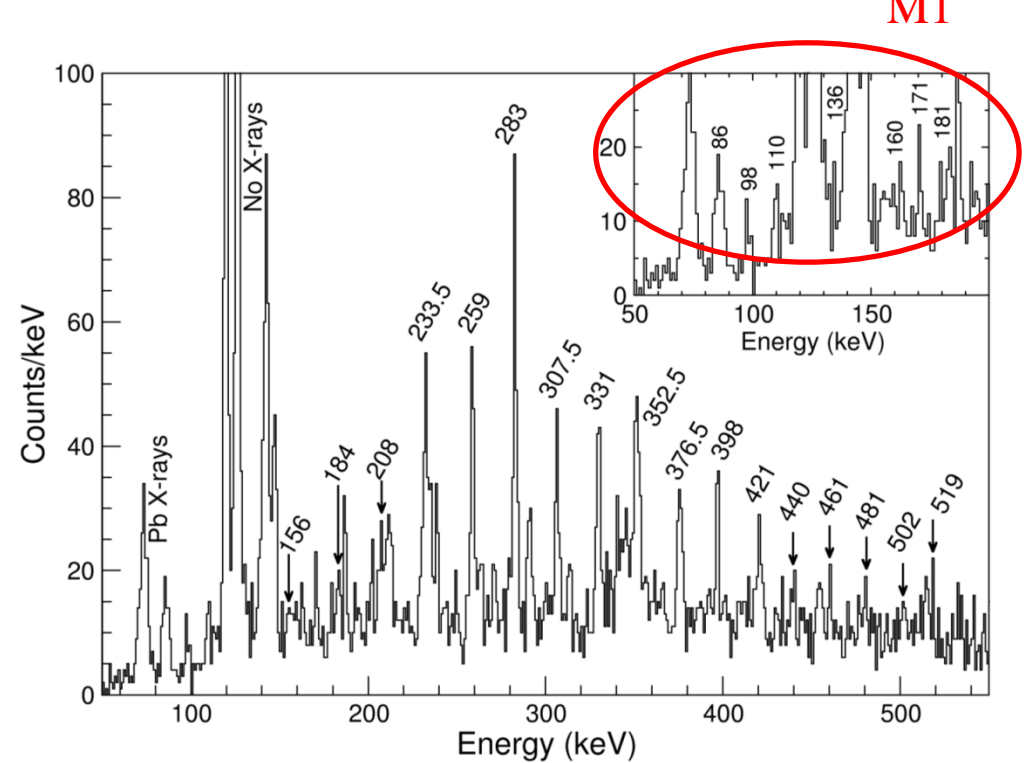


^{254}No ($Z=102$), ^{252}Fm ($Z=100$) and ^{250}Cf ($Z=98$)
with $N=152$
seem to be more stable than their neighbors

Level scheme of ^{253}No (151 neutrons)



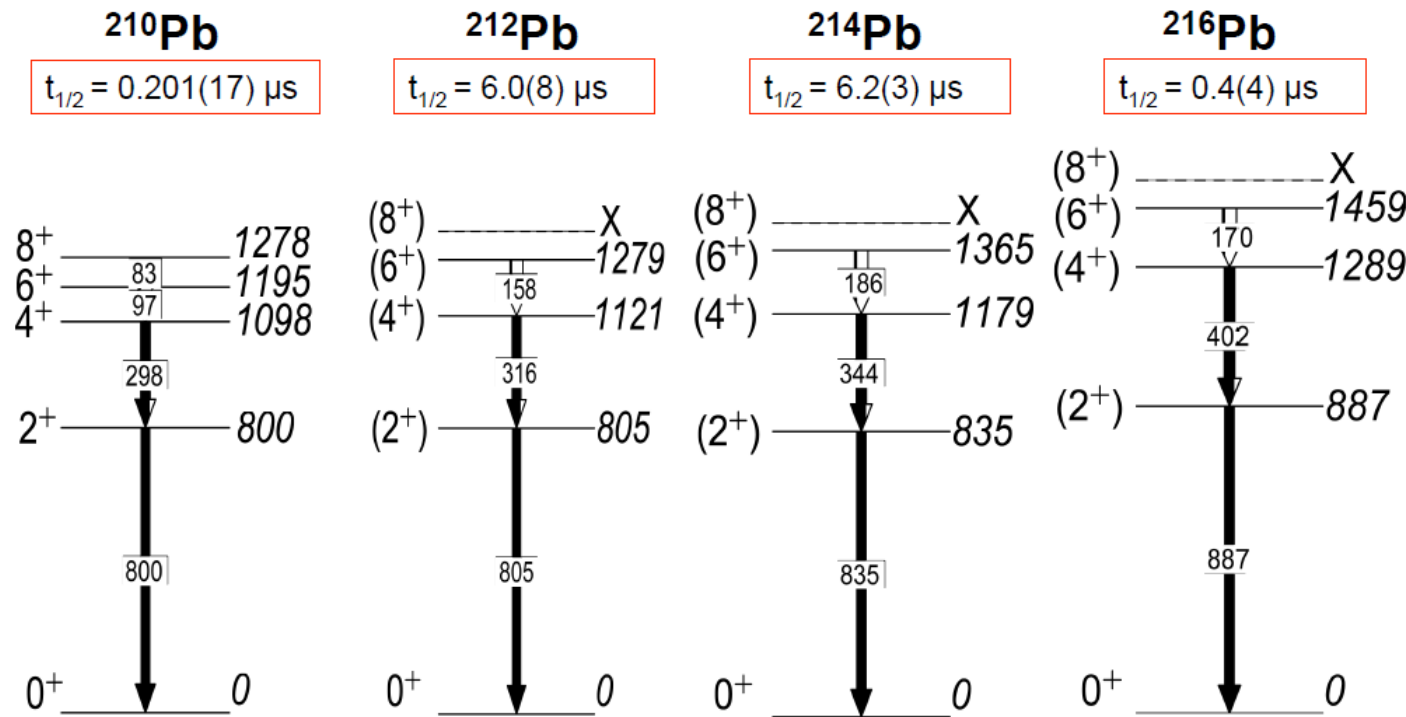
- ❖ ground state $9/2^-$
- ❖ excited state $7/2^+$
- ❖ rotational band observed at Gammasphere & JUROGAM



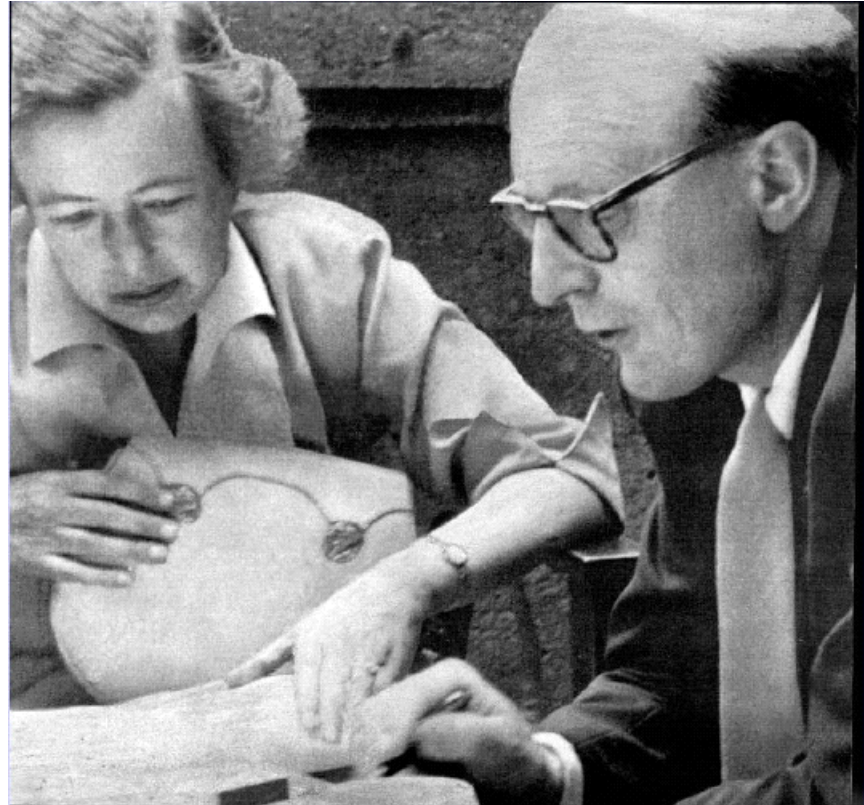
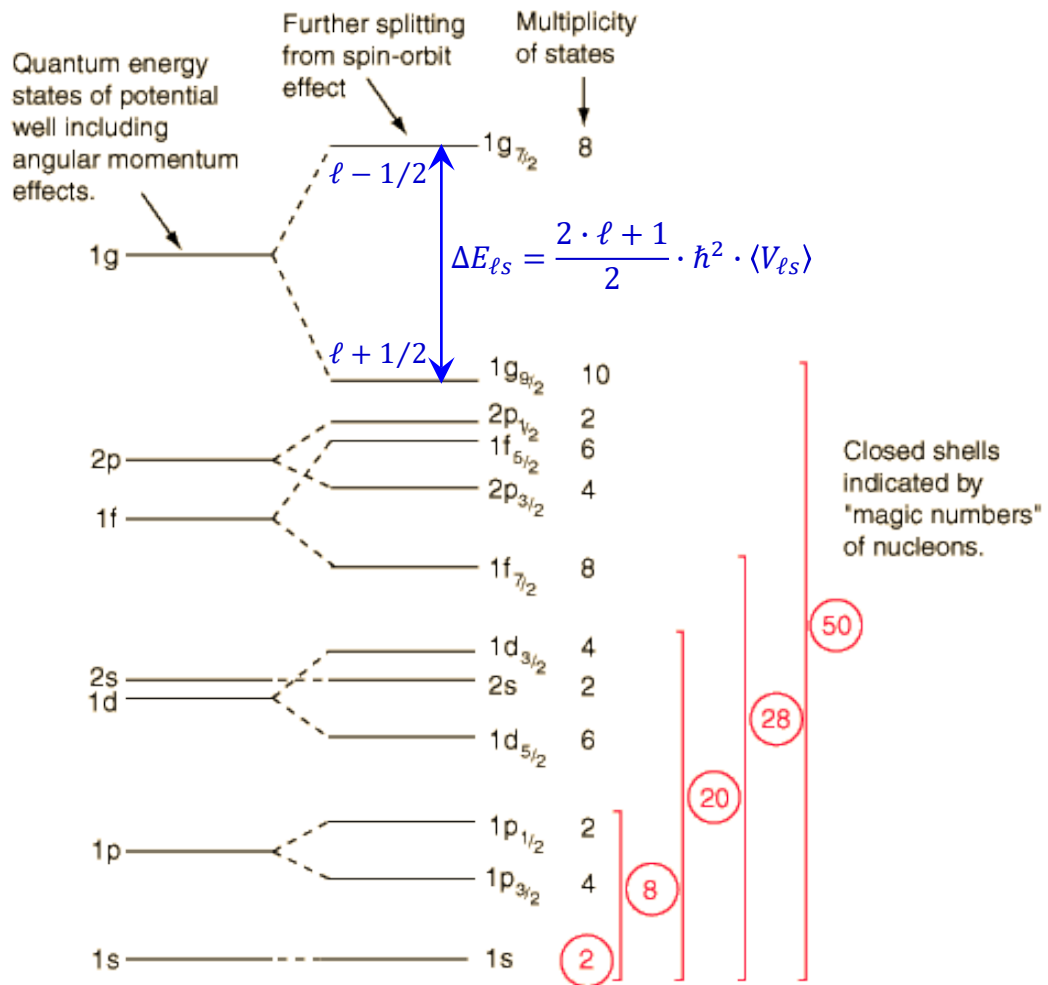
Level schemes in neutron-rich Pb isotopes

Pb205 1.53E+7 y 5/2- * EC	Pb206 0+ 24.1	Pb207 1/2- * 22.1	Pb208 0+ 52.4	Pb209 3.253 h 9/2+ β^-	Pb210 22.3 y 0+ β^-, α	Pb211 36.1 m 9/2+ β^-	Pb212 10.64 h 0+ β^-	Pb213 10.2 m (9/2+) β^-	Pb214 26.8 m 0+ β^-	Pb215 36 s (5/2+) β^-	Pb216	Pb217	Pb218
---------------------------------------	---------------------	----------------------------	---------------------	---------------------------------------	--	--------------------------------------	-------------------------------------	--	------------------------------------	--------------------------------------	-------	-------	-------

↔
 $g_{9/2}$



The magic numbers near stable nuclei



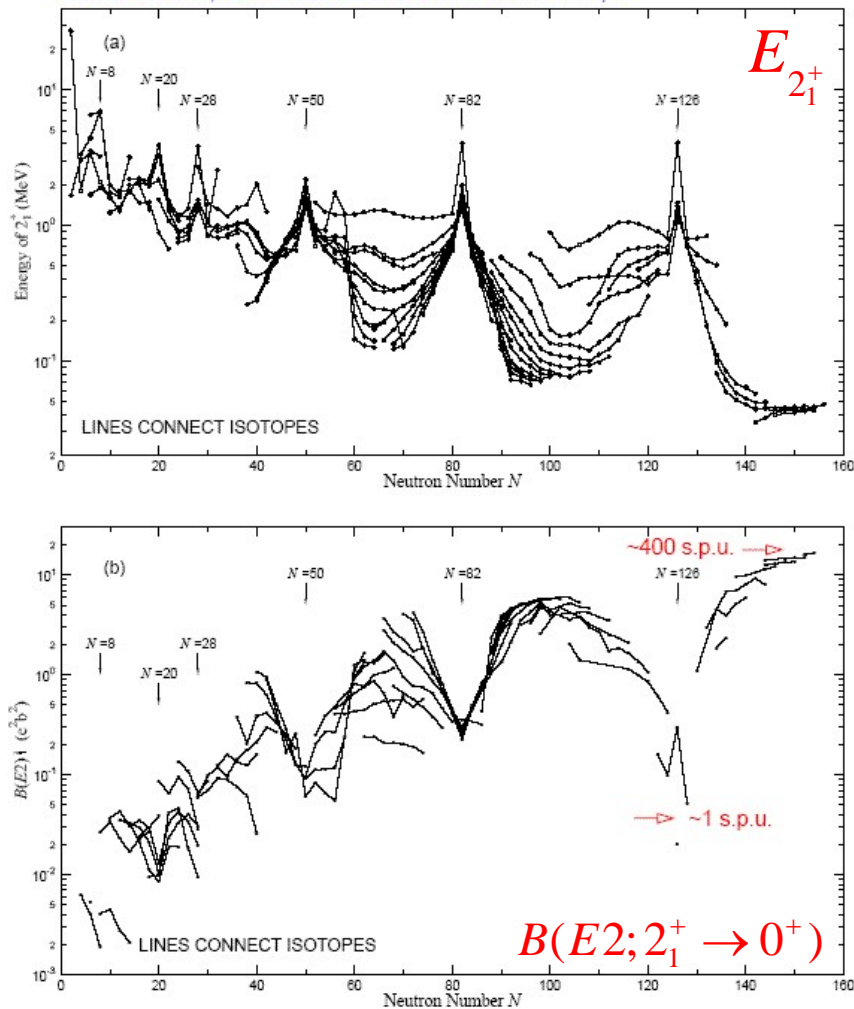
Maria Goeppert-Mayer (1906-1972)
Hans Jensen (1907-1973)

*magic numbers with constant shell closures
are not so robust, as we thought.*

Nuclear shell structure

experimental hints for magic numbers

S. Raman et al., Atomic Data & Nuclear Data Tables 78, 1



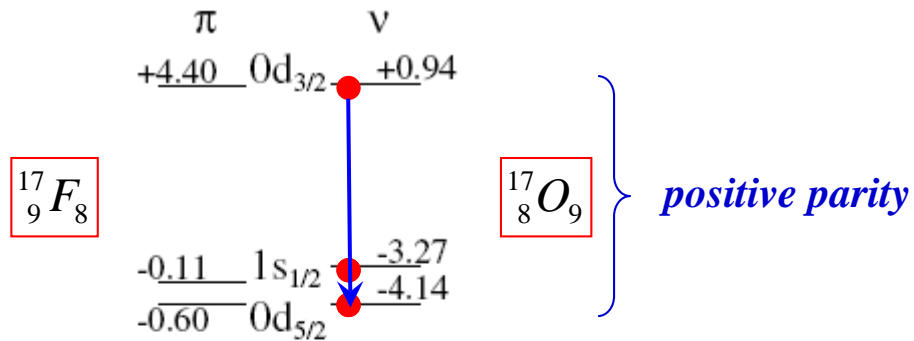
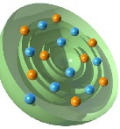
nuclei with magic numbers

neutron / proton:
high energies for 2_1^+ states

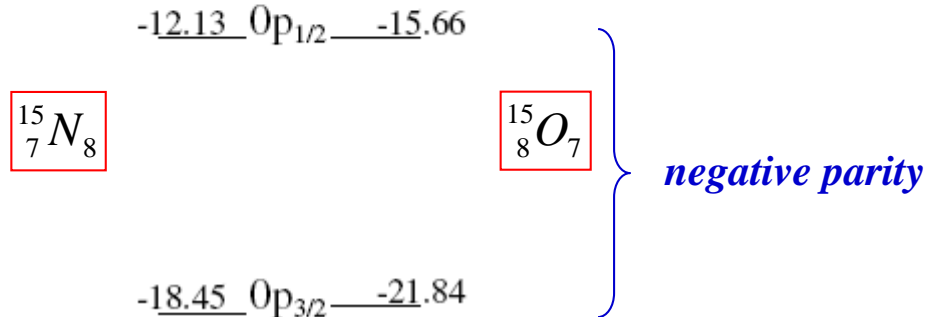
small $B(E2; 2_1^+ \rightarrow 0^+)$ values
transition probabilities are measured in
Weisskopf units (spu)

What happens far away from the valley of stability?

Extreme single-particle shell model



$\boxed{^{16}_8 O_8}$



proton neutron

energies of shell closure:

$$BE(^{17}_9 F_7) - BE(^{16}_8 O_8) = E(0 d_{5/2})$$

$$BE(^{15}_7 N_8) - BE(^{16}_8 O_8) = -E(0 p_{1/2})$$

$$\begin{aligned} E(0 d_{5/2}) - E(0 p_{1/2}) &= BE(^{17}_9 F_8) + BE(^{15}_7 N_8) - 2 \cdot BE(^{16}_8 O_8) \\ &= -11.526 \text{ MeV} \end{aligned}$$

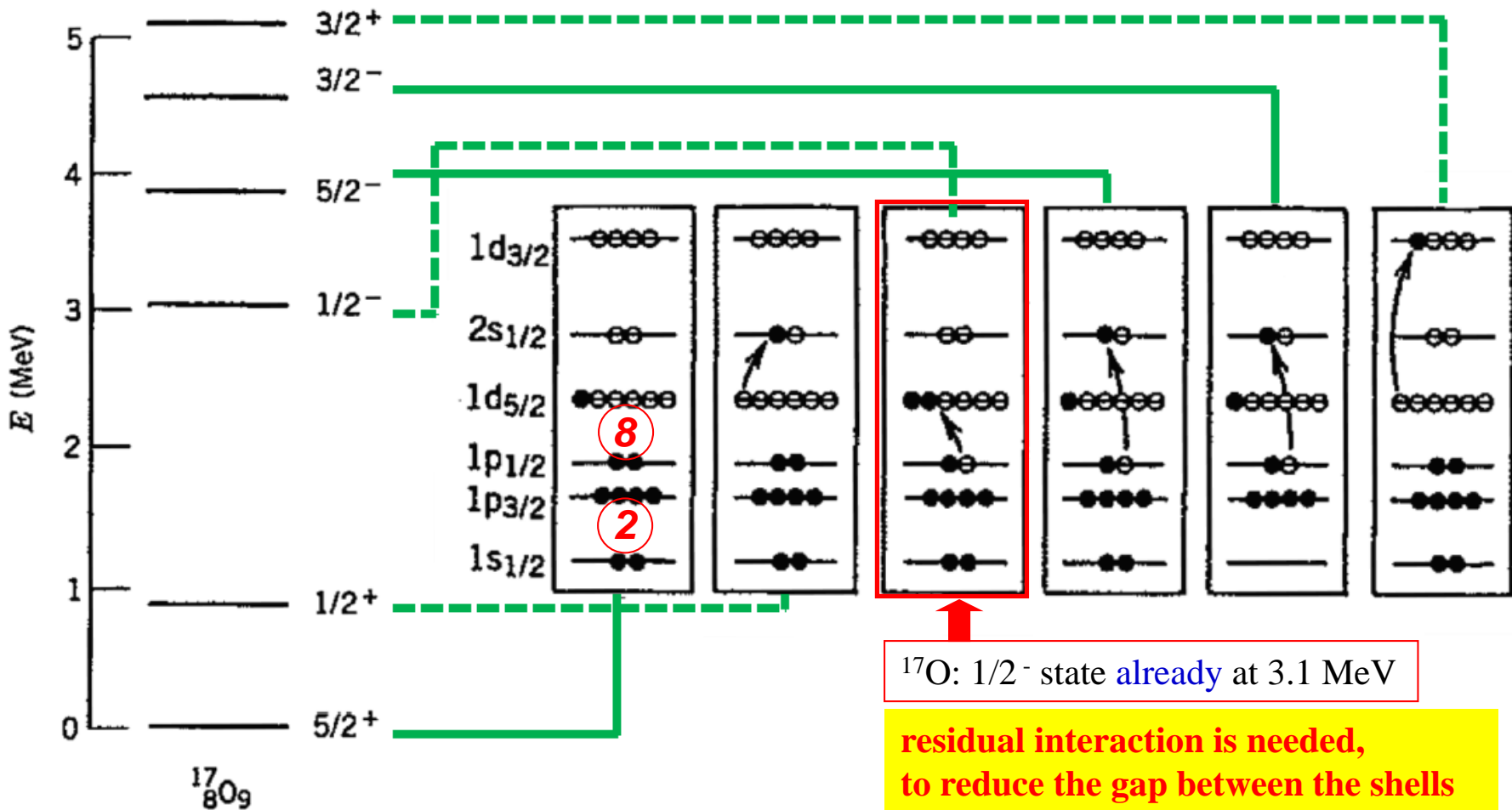
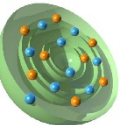
$$BE(^{17}_8 O_9) - BE(^{16}_8 O_8) = E(0 d_{5/2})$$

$$BE(^{15}_8 O_7) - BE(^{16}_8 O_8) = -E(0 p_{1/2})$$

$$\begin{aligned} E(0 d_{5/2}) - E(0 p_{1/2}) &= BE(^{17}_8 O_9) + BE(^{15}_8 O_7) - 2 \cdot BE(^{16}_8 O_8) \\ &= -11.519 \text{ MeV} \end{aligned}$$

good prediction of
spin
parity $\pi = (-1)^\ell$
magnetic moment

Single-particle energies



Single-particle states observed in odd- A nuclei (especially one nucleon + doubly magic nucleus as ^4He , ^{16}O , ^{40}Ca) are characterized by the single-particle energies in the shell model picture.

Classic example of anomaly



Several anomalies were observed in shell structures of exotic nuclei: proton-rich or neutron-rich

Classic example : ^{11}Be

3.09MeV

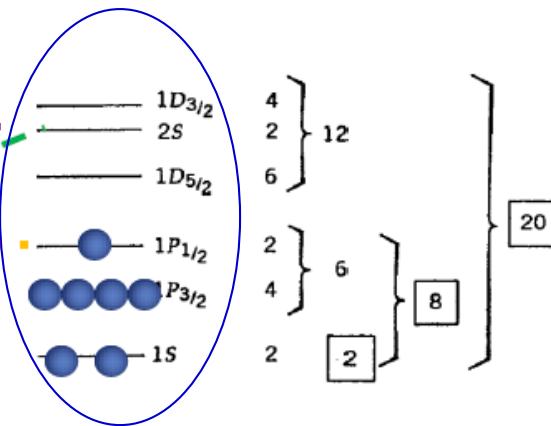
$1/2^+$

gs

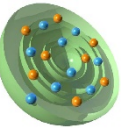
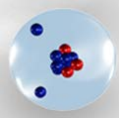
$1/2^-$

$^{13}\text{C}_7$ (stable)

expected !



The $2s_{1/2}$ orbital (parity +) and the $1p_{1/2}$ orbital (parity -) are inverted ?? (**parity inversion**)



Formation of halos and the s-orbital

The **s** component in the ground state is essential for creating a halo structure.

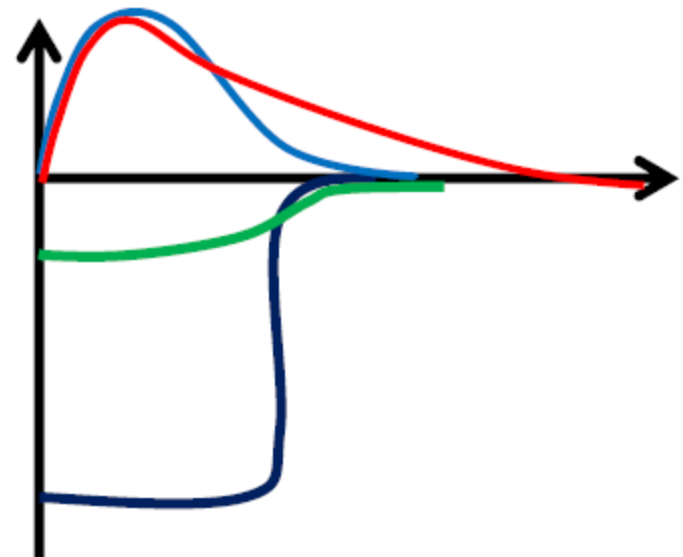
Schrödinger equation: $\left[-\frac{\hbar^2}{2 \cdot \mu} \nabla^2 + V(r) \right] \Psi(r) = E \Psi(r)$ $\Psi(r) = u_{nl}(r) \cdot Y_{lm}(\theta, \varphi)$

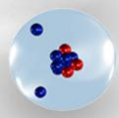
$$\frac{d^2u}{dr^2} + \frac{2}{r} \frac{du}{dr} + \left[\frac{2 \cdot \mu}{\hbar^2} (E - V(r)) - \frac{\ell \cdot (\ell + 1)}{r^2} \right] u(r)$$

centrifugal barrier ($\ell = 0$ for s-wave)

neutron-rich nuclei (^{11}Be , ^{11}Li)

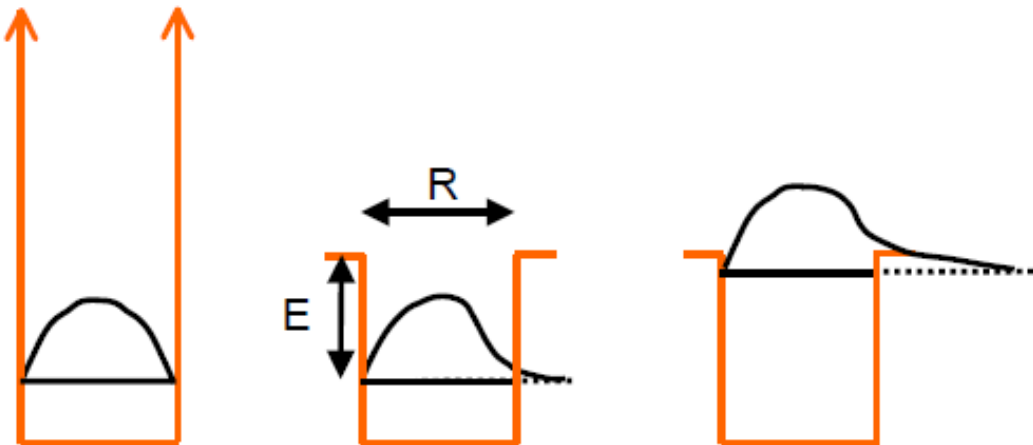
- instable: flat nuclear potential
- the wave function is extended
- for **s-orbitals**, the radial extension
is not blocked by the centrifugal barrier
(**halo**)





Halo nuclei

What can we expect at the neutron-dripline?



wave function outside of the potential

$$\Psi(r) \propto \frac{e^{-\kappa r}}{r}$$

$$\kappa^2 = \frac{2 \cdot \mu \cdot E}{\hbar^2} \approx 0.05 \cdot E(\text{MeV}) \quad [\text{fm}^{-2}]$$

$$\langle r^2 \rangle = \frac{\int r^4 dr (e^{-\kappa \cdot r} / \kappa \cdot r)^2}{\int r^2 dr (e^{-\kappa \cdot r} / \kappa \cdot r)^2}$$

The smaller the binding energy, the more extended is the wave function

$$\langle r^2 \rangle = \frac{1}{2 \cdot \kappa^2} \cdot (1 + \kappa \cdot R) \approx \frac{\hbar^2}{4 \cdot \mu \cdot S_n}$$

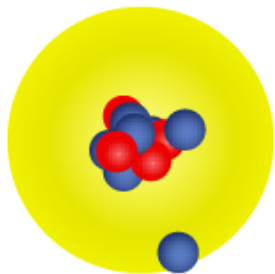
E	κ^2	κ	$1/\kappa \sim r$
7 MeV	0.35 fm ⁻²	0.6 fm ⁻¹	1.7 fm
1 MeV	0.05 fm ⁻²	0.2 fm ⁻¹	4.5 fm
0.1 MeV	0.005 fm ⁻²	0.07 fm ⁻¹	14 fm

Halo nuclei



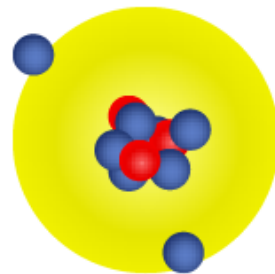
Anomalies of the shell structure was first observed in

^{11}Be ($Z=4$, $N=7$) and ^{11}Li ($Z=3$, $N=8$),
the most famous one-neutron halo and two-neutron halo-nuclei.

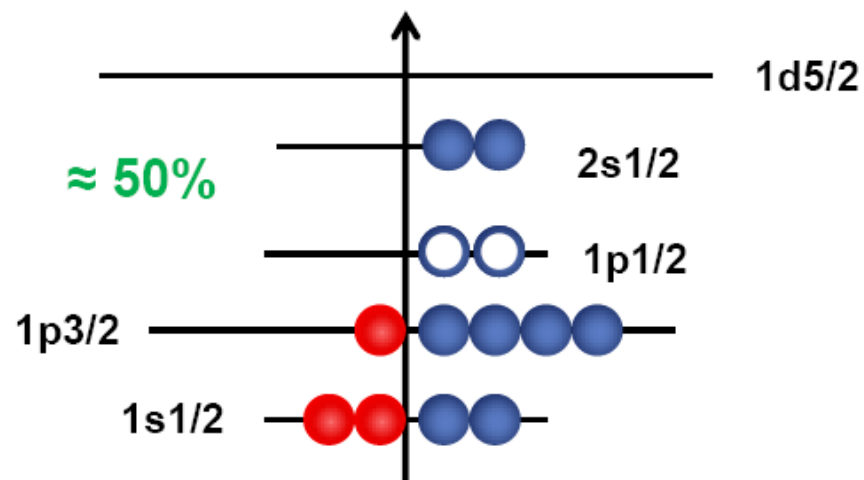
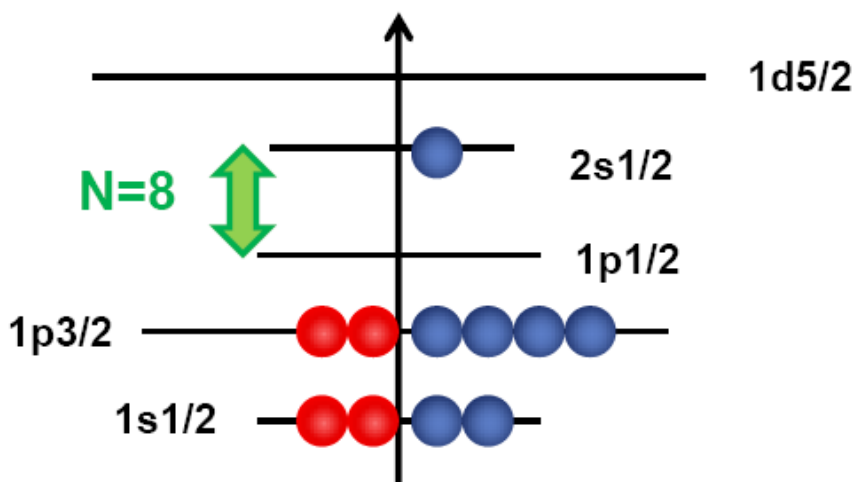


ground-state
spin (J^π)

$1/2^+$



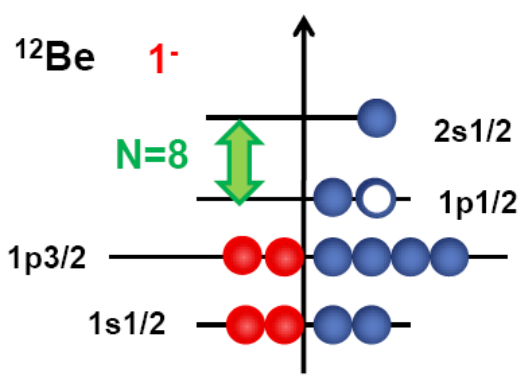
$3/2^-$



Change of the magic number near N=8: ^{12}Be

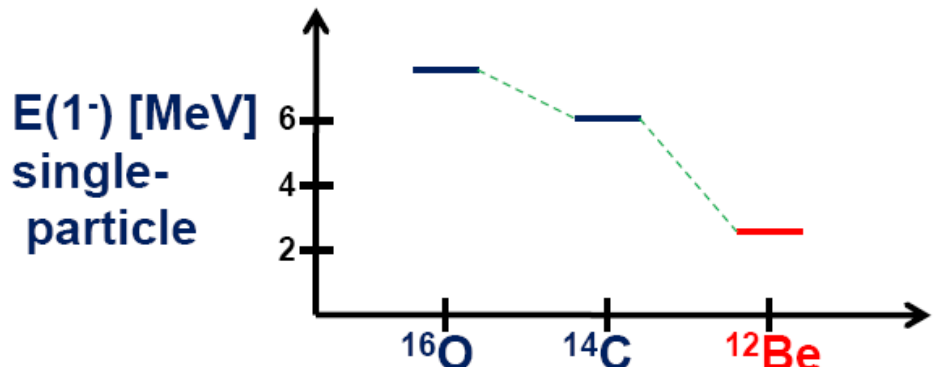
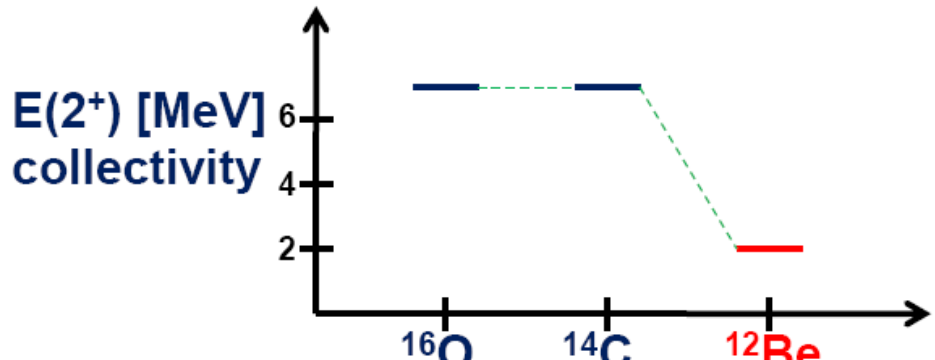


				^{17}F	^{18}F	^{19}F
$Z = 8$	^{13}O	^{14}O	^{15}O	^{16}O	^{17}O	^{18}O
	^{12}N	^{13}N	^{14}N	^{15}N	^{16}N	^{17}N
^9C	^{10}C	^{11}C	^{12}C	^{13}C	^{14}C	^{15}C
^8B		^{10}B	^{11}B	^{12}B	^{13}B	^{14}B
^7Be		^9Be	^{10}Be	^{11}Be	^{12}Be	^{14}Be
^6Li	^7Li	^8Li	^9Li	^{10}Li		
						$N = 8$



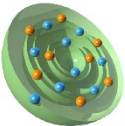
Is the magic number changed only in halo nuclei ?
No! It holds also for ^{12}Be .

This observation indicates a universal evolution of the shell structure.



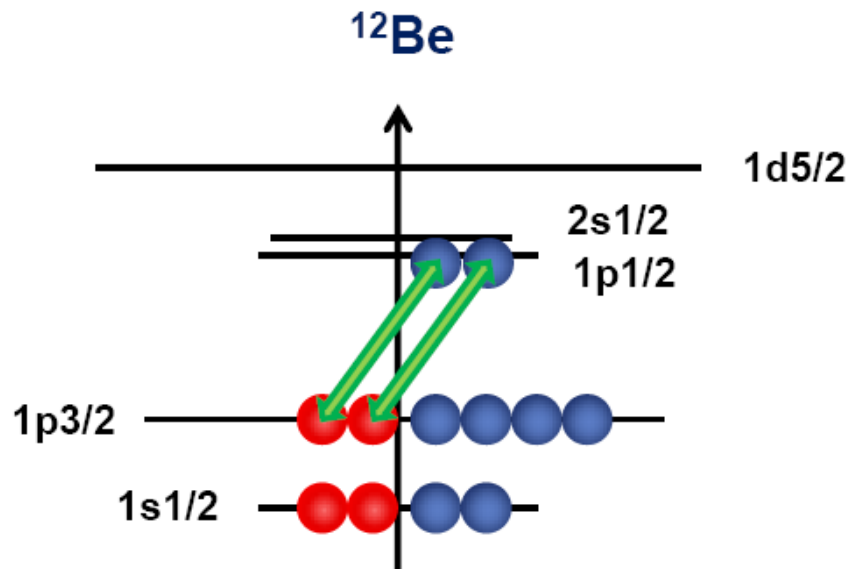
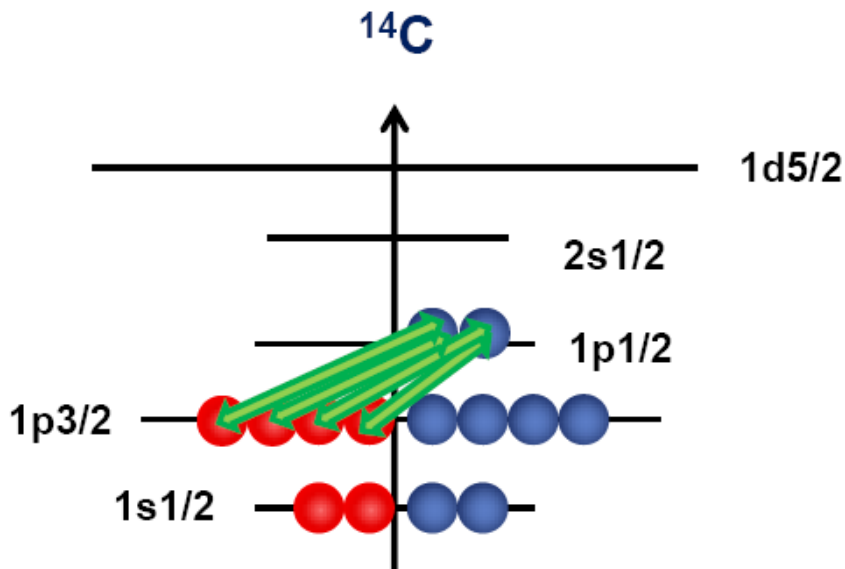
Simplified picture of monopole effects of the tensor force

nucleon-nucleon residual interaction



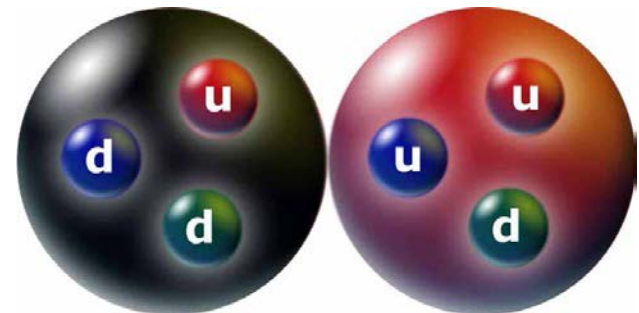
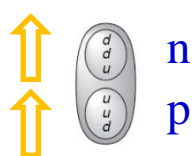
The specific **proton-neutron interaction** (**monopole term of the tensor-force**) can change the single-particle order, depending on the proton-neutron ratio of the nucleus.

The strong attractive p-n force between $J_>$ and $J_<$ orbitals ($\begin{cases} >: \ell + 1/2 \\ <: \ell - 1/2 \end{cases}$ for example, $\pi p_{3/2}$ and $\nu p_{1/2}$)



The deuteron

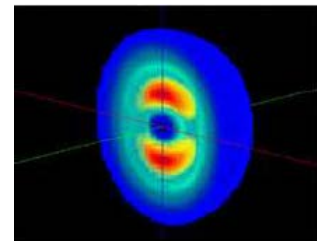
mass (MeV/c^2)	1875.61
charge (e)	1
I^π	1^+
binding energy (MeV)	2.2245
magnetic moment (μ_N)	0.8574
quadrupole moment (b)	0.0029



The deuteron is an ideal candidate for tests of our basic understanding of nuclear physics

Deuteron: quadrupole moment

- The measured **nuclear spin** of the deuteron is **$J = 1$**
- The **parity** of the deuteron is **positive**, only even **angular momenta $\ell = 0$** and **$\ell = 2$** .
- The **magnetic moment** of the deuteron yields to $\mu = 0.8574 \cdot \mu_K$ The angular momentum has to **4%** the value of **$\ell = 2$**
- The deuteron is **not spherical**.
It has an experimentally determined **quadrupole moment** of **$Q = 0.00282$ eb**.



A free neutron and a free proton have no electric quadrupole moment.

The deuteron can only possess a quadrupole moment because of its angular momentum of **$\ell = 2$** .

$$Q_{zz} = \int \rho(\vec{r}) \cdot r^2 \cdot (3 \cdot \cos^2 \theta - 1) d\tau$$

A pure $\ell = 0$ wave function has a vanishing quadrupole moment, because of its rotational symmetry.

The nuclear force is spin dependent !

The nuclear forces must raise a torsional moment, that depend on the radius r and the angle θ .

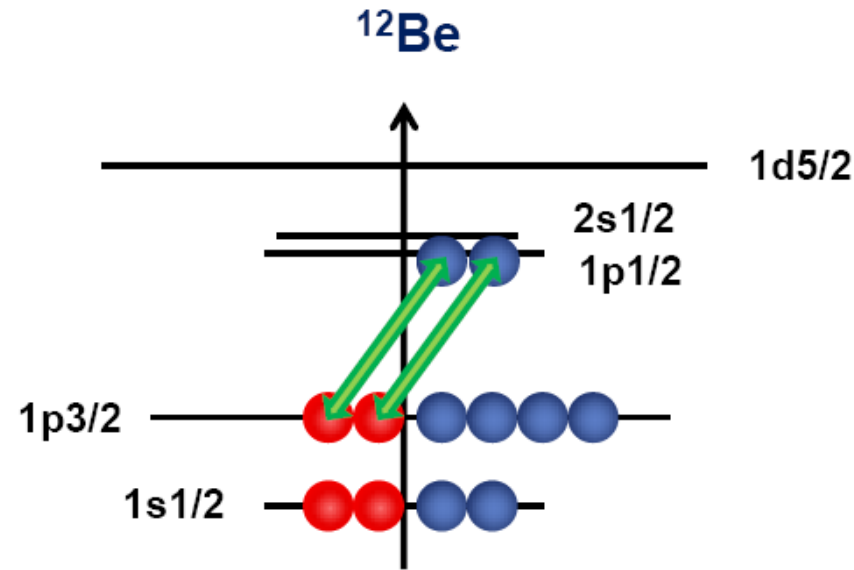
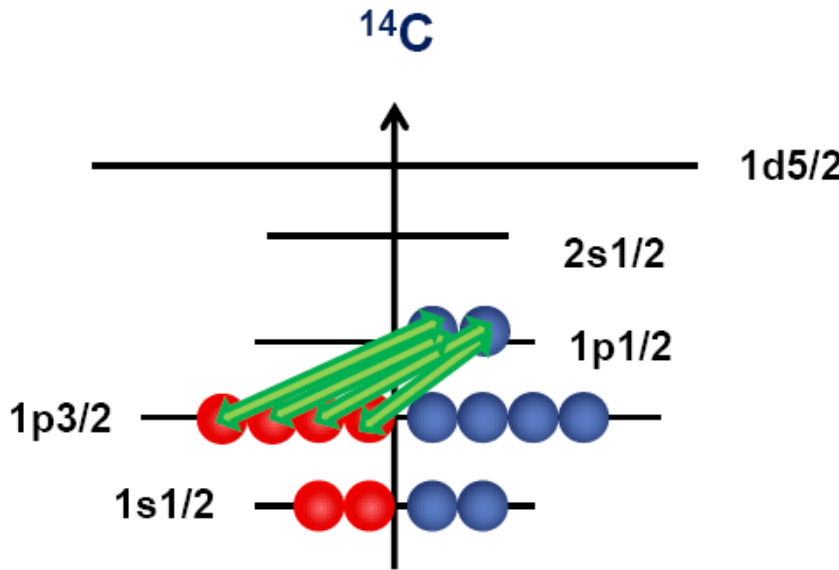
If the nuclear force depends on r and θ , then there is a non-central force component a **Tensor force**

Simplified picture of monopole effects of the tensor force

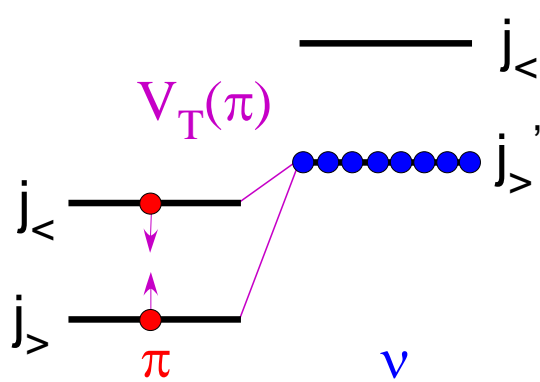
nucleon-nucleon residual interaction

The example shows the proton configuration ($0p_{3/2}$) of $^{14}\text{C}_8$. The more protons are in $0p_{3/2}$ orbital, the more the $0p_{1/2}$ neutron orbital will be attracted and the shell closure at N=8 develops.

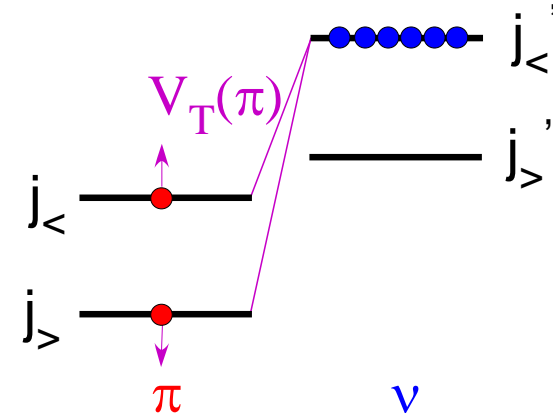
For $^{12}\text{Be}_8$ the proton orbital $0p_{3/2}$ will be emptied, the interaction is weaker and the neutron orbital $0p_{1/2}$ will be lifted.



The effect of the tensor force on the ℓs -coupling



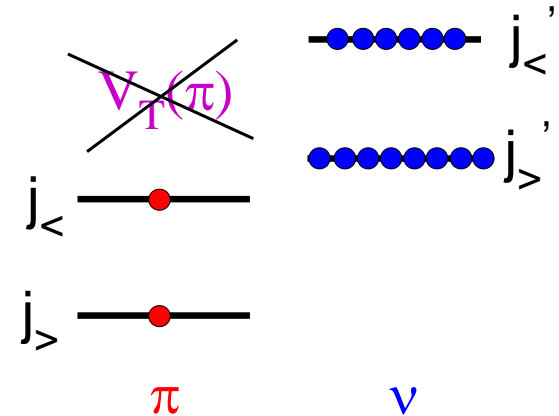
V_T reduces ls-splitting.



V_T enhances ls-splitting.

1. $j_< - j'_<$ or $j_< - j'_>$: **repulsion**
2. $j_< - j'_>$: **attraction**
3. If both $j'_<$ and $j'_>$ orbitals are fully occupied the tensor force does not act.

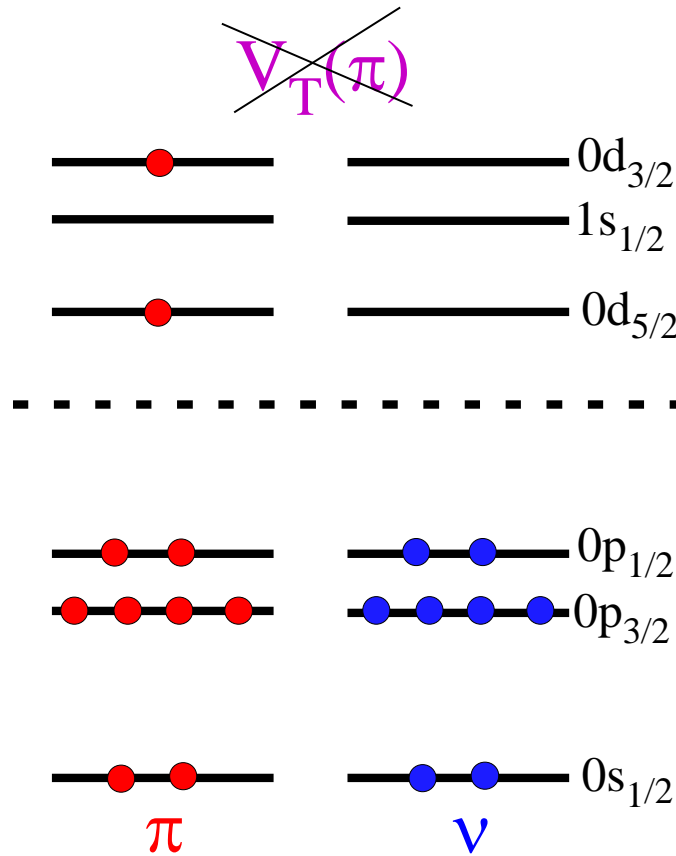
cf. Bouyssy et al. PRC **36** (1987) 380
Otsuka et al. PRL **95** (2005) 232502



V_T does not act.

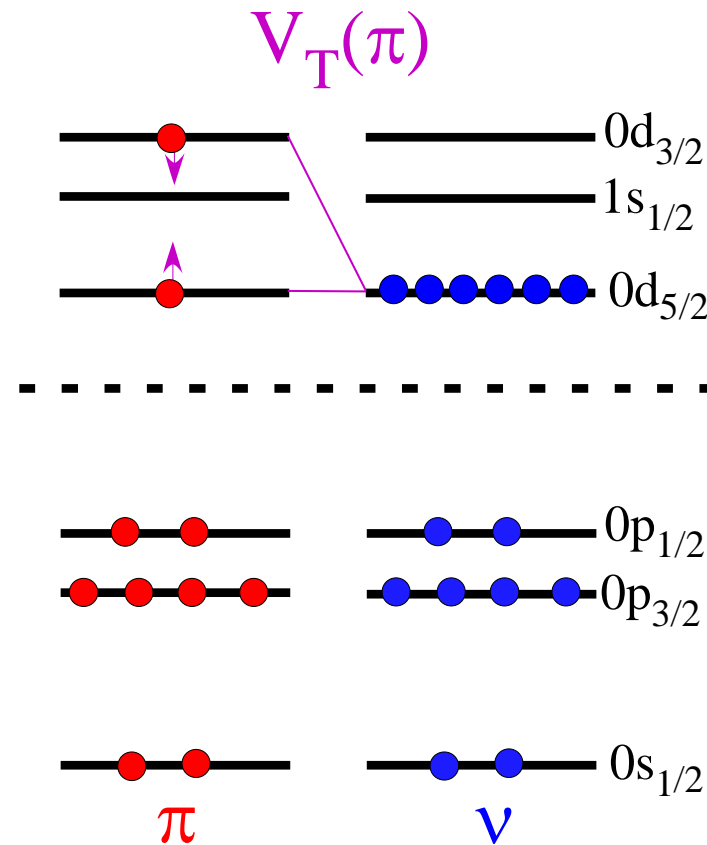
The effect of the tensor force on the ℓs -coupling

$^{17}\text{F}({}^{16}\text{O}+\text{p})$



The tensor force does not act

$^{23}\text{F}({}^{22}\text{O}+\text{p})$



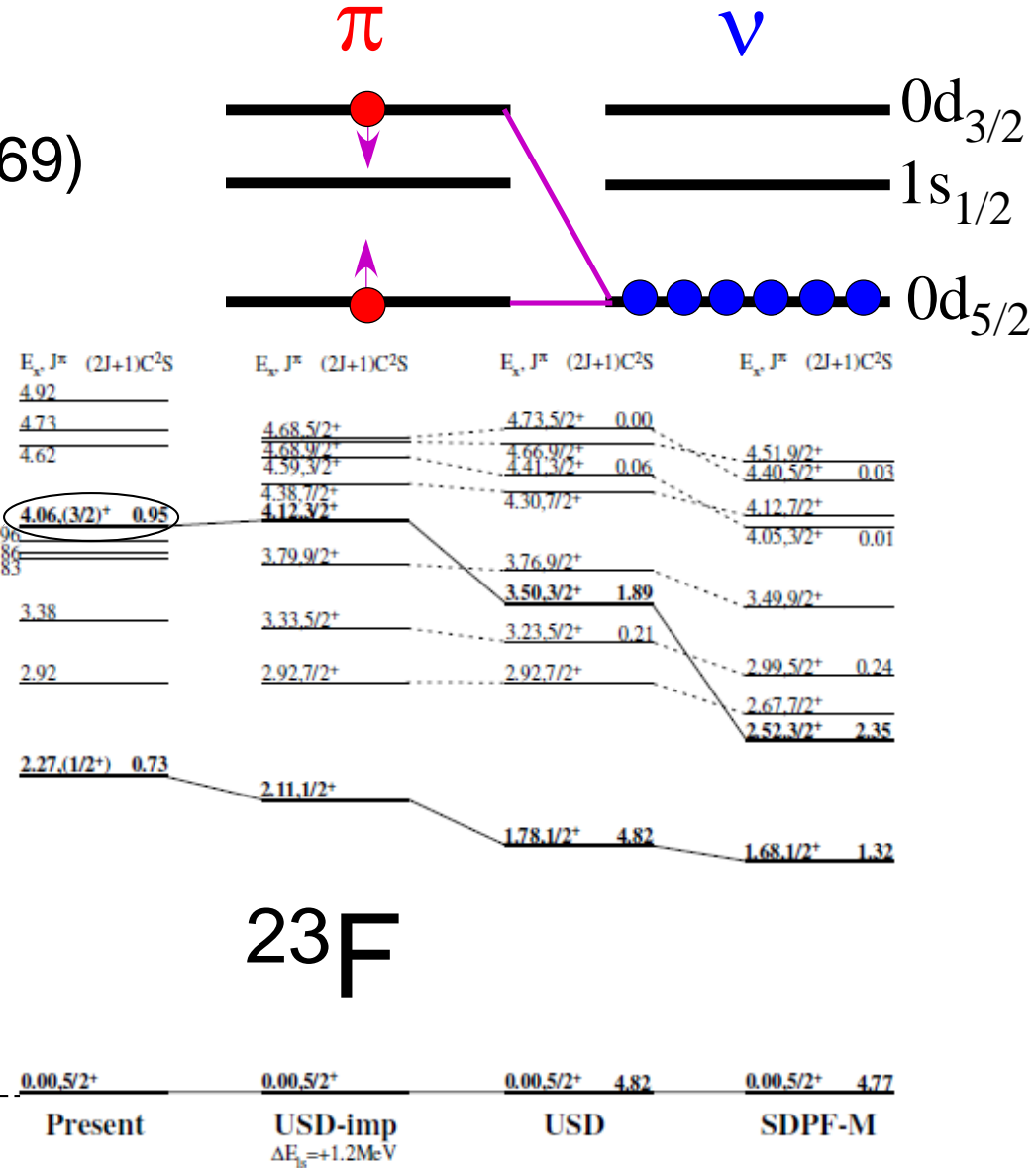
The tensor force reduces the ℓs -splitting

Michimasa et al.
(from NPA 787 (2007) 569)

$3/2^+$ ————— 5 MeV

$5/2^+$ —————
 17F

Figure 3. Level schemes in ^{23}F , together with the shell model calculations using USD [9] and SDPF-M [10] effective interactions. The level scheme labeled by USD-imp was obtained based on the USD by widening the single-particle energy gap between $\pi d_{5/2}$ and $\pi d_{3/2}$ by +1.2 MeV.



Application to other shells

β -DECAY SCHEMES OF VERY NEUTRON-RICH SODIUM ISOTOPES AND THEIR DESCENDANTS

D. GUILLEMAUD-MUELLER *, C. DETRAZ *, M. LANGEVIN and F. NAULIN

Institut de Physique Nucléaire, BP 1, F-91406 Orsay, France

M. DE SAINT-SIMON, C. THIBAULT and F. TOUCHARD

Laboratoire René Bernas du Centre de Spectrométrie Nucléaire et de Physique des Particules, BP 1, F-91406 Orsay, France

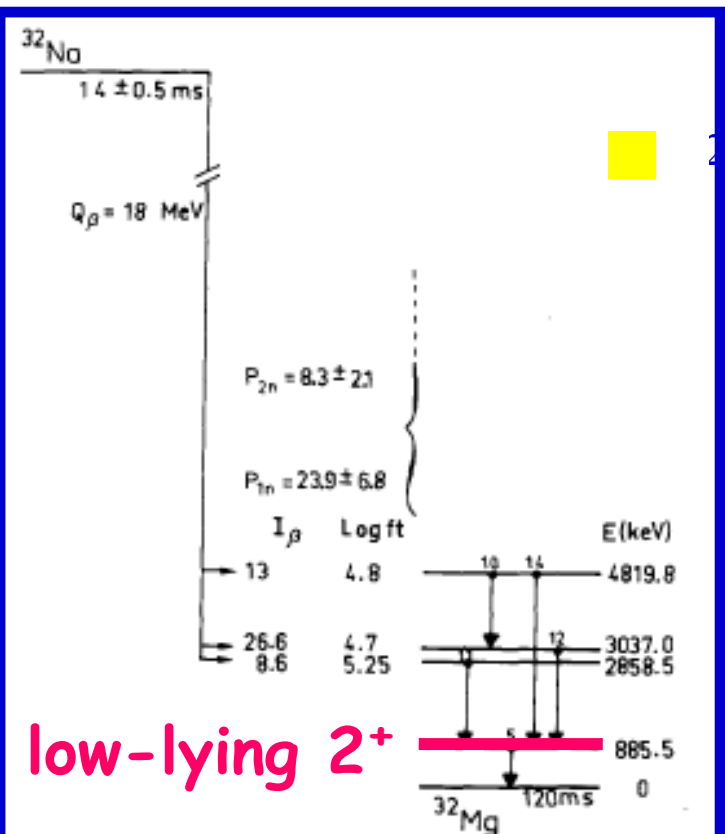
and

M. EPHERRÉ

Laboratoire René Bernas and CERN, Division EP, CH-1211 Genève 23, Switzerland

Received 6 February 1984

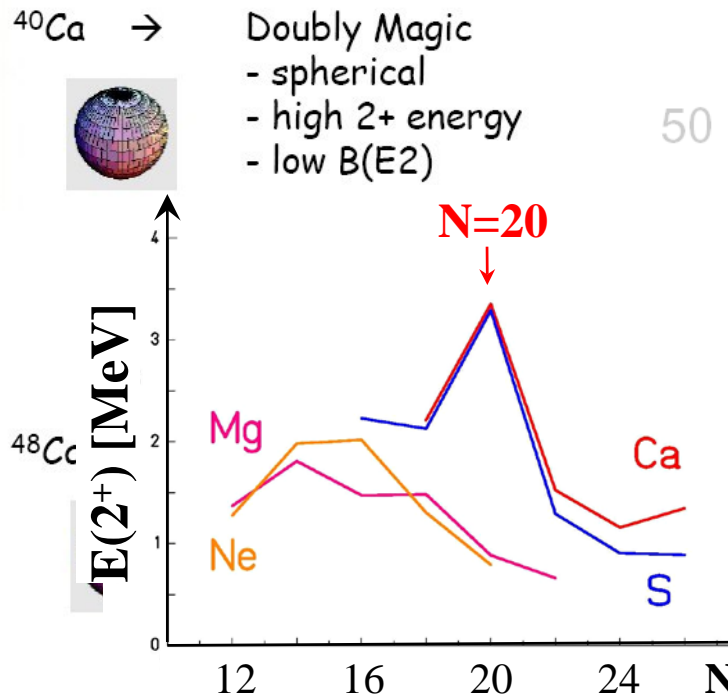
Abstract: The γ -activities from the β -decay of Na isotopes up to ^{32}Na were measured after fragmentation and analysed through mass-spectrometry techniques. The I_{γ} intensities, the β -delayed γ -activities and the I_{β} intensities are measured. Decay schemes are proposed. The location of the first 2^+ level of ^{32}Mg , the occurrence of a nuclear



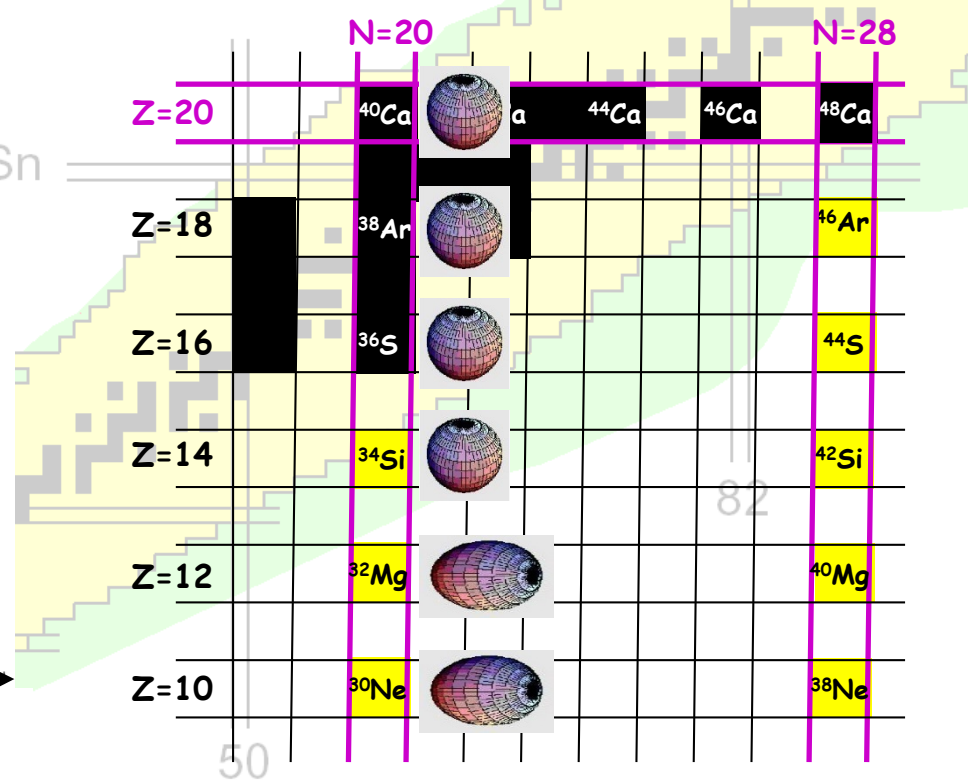
Nuclear shell model

Experimental evidence of the magic numbers

Status of the art...



50 Sn



Evidence of the nuclear shell model:

high energies of the 2_1^+ states

for nuclei with magic numbers

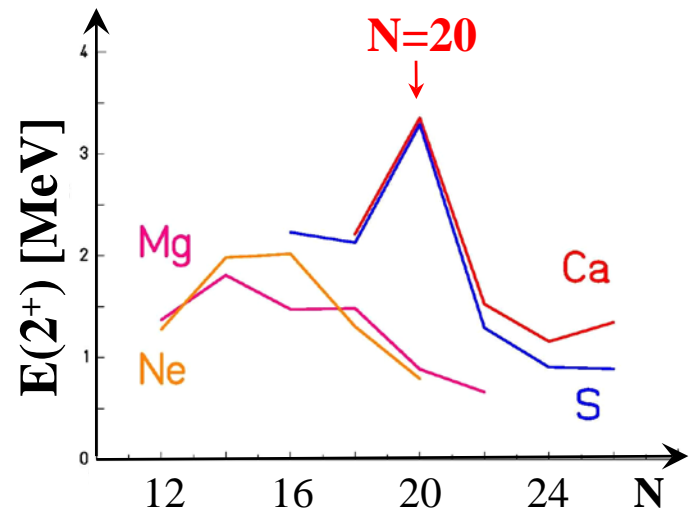
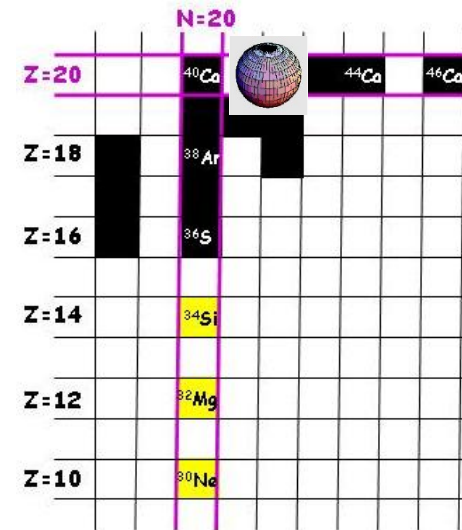
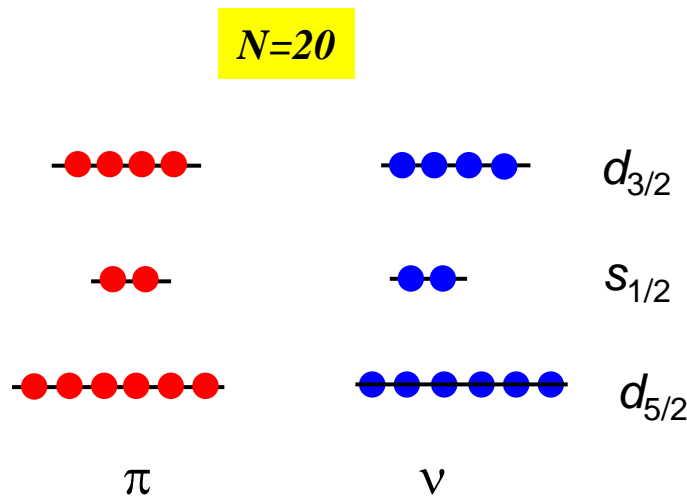
Monopole-interaction of the tensor force

Experimental evidence of the magic number

N=20

$^{40}_{20}Ca_{20}$

— $f_{7/2}$

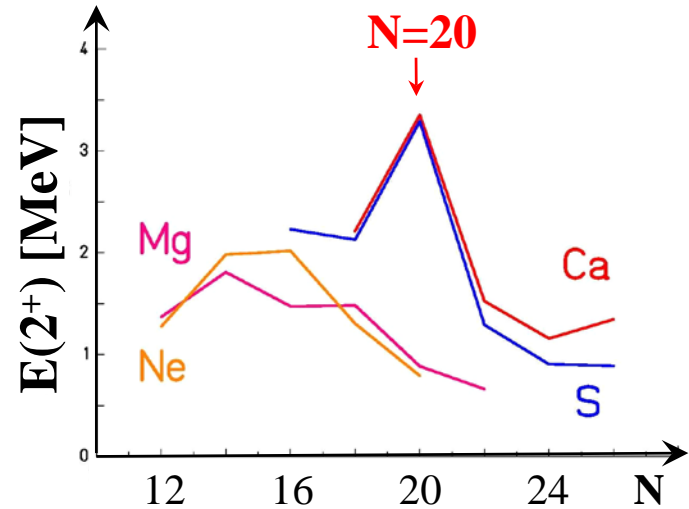
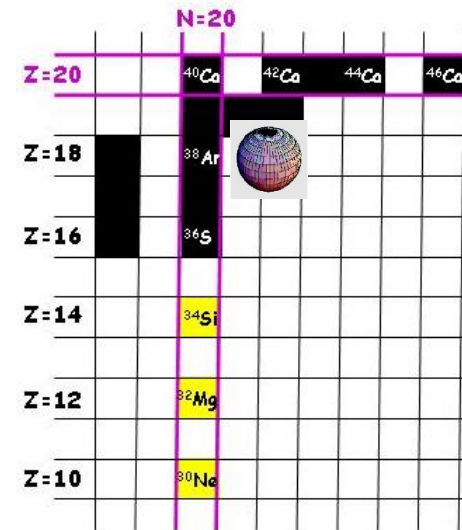
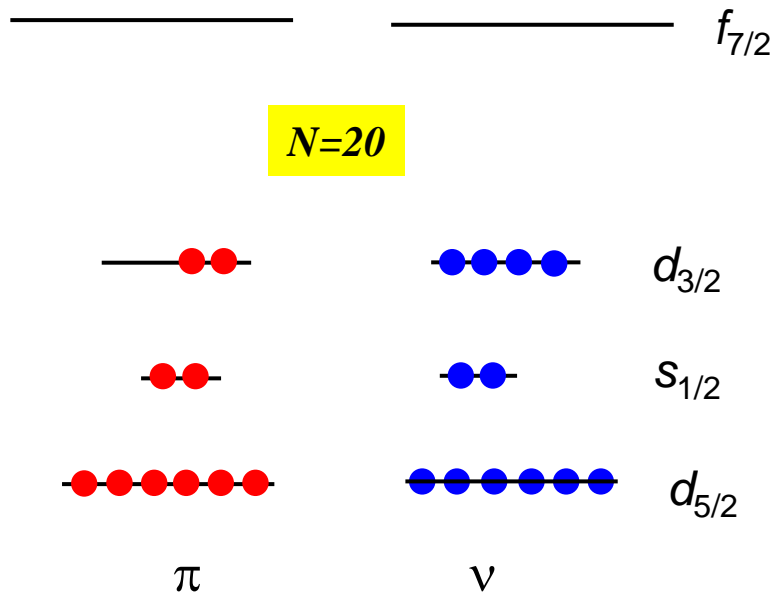


Monopole-interaction of the tensor force

Experimental evidence of the magic number

N=20

$^{38}_{18}Ar_{20}$

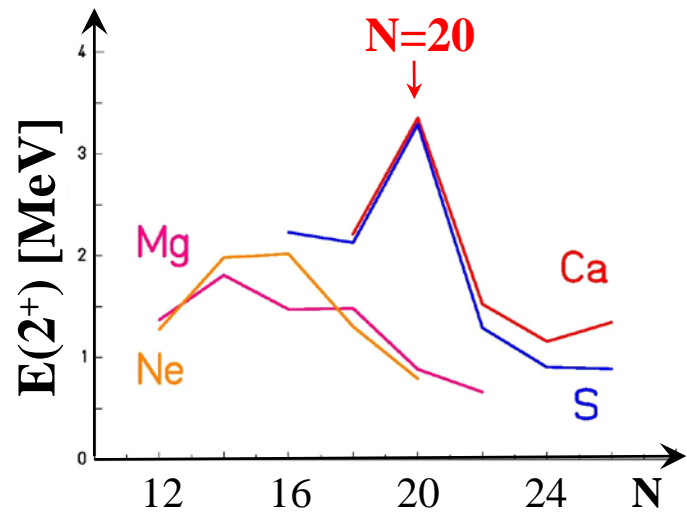
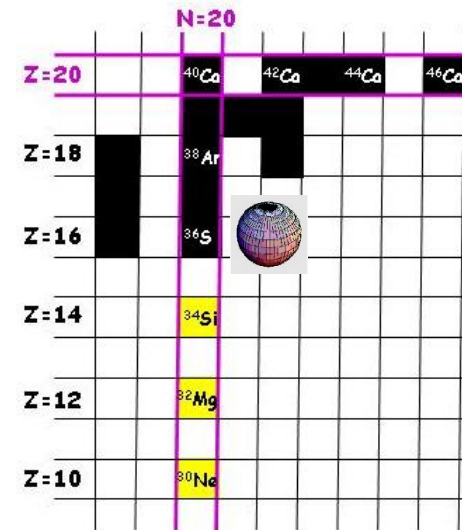
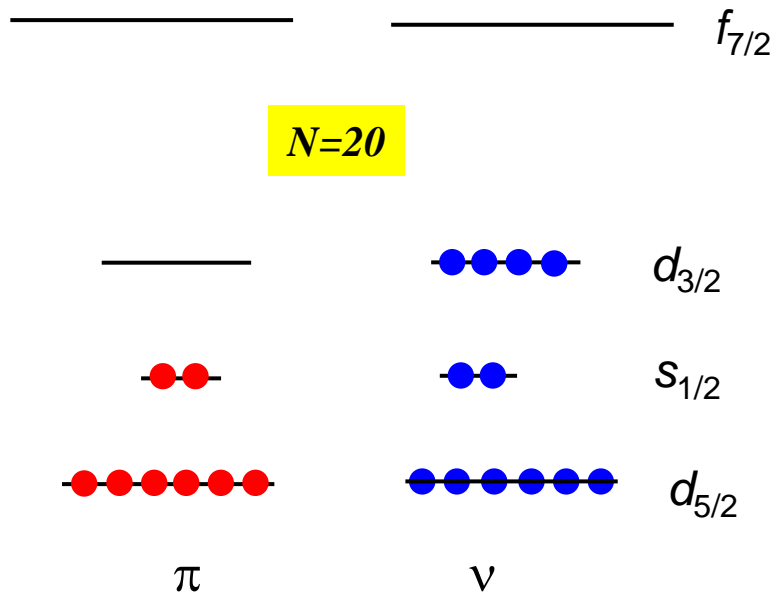


Monopole-interaction of the tensor force

Experimental evidence of the magic number

N=20

$^{36}_{16}S_{20}$

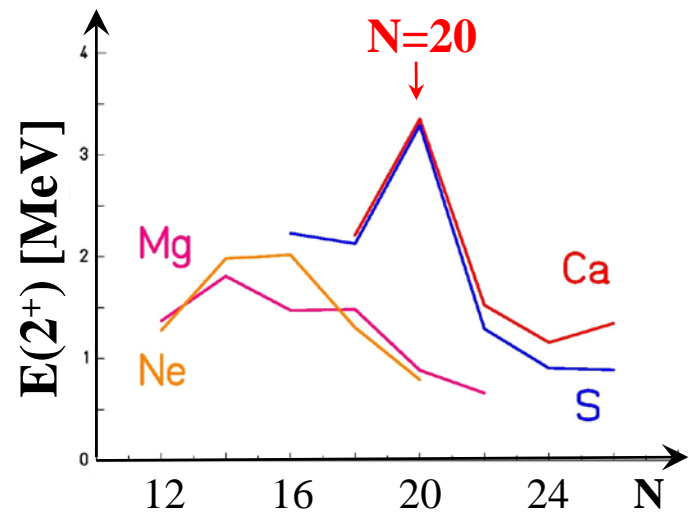
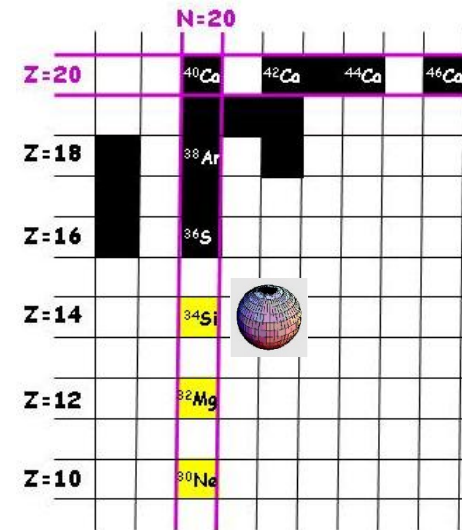
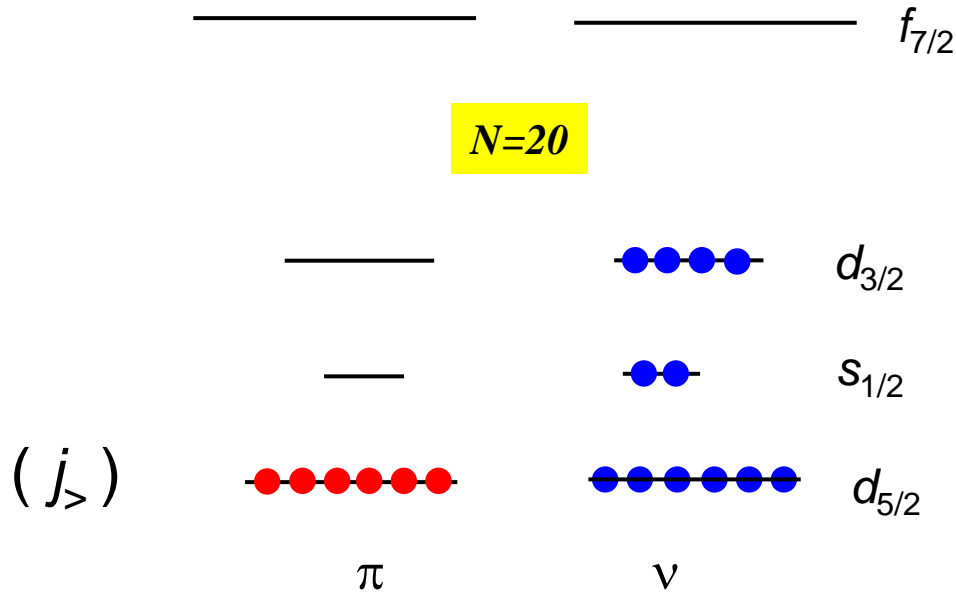


Monopole-interaction of the tensor force

Experimental evidence of the magic number

N=20

$^{34}_{14}Si_{20}$

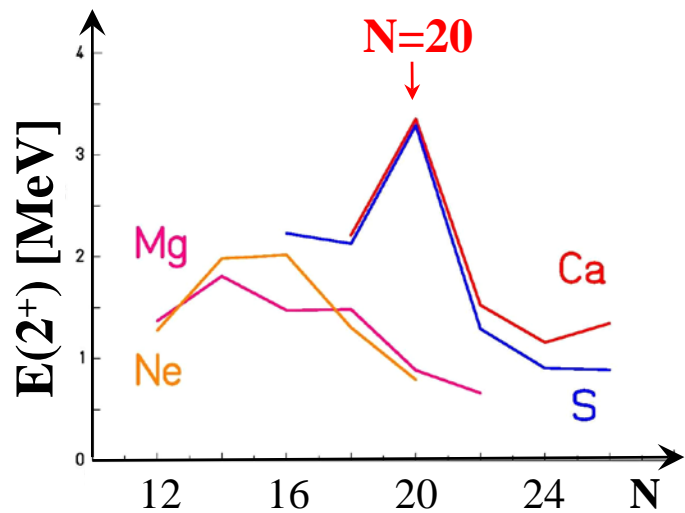
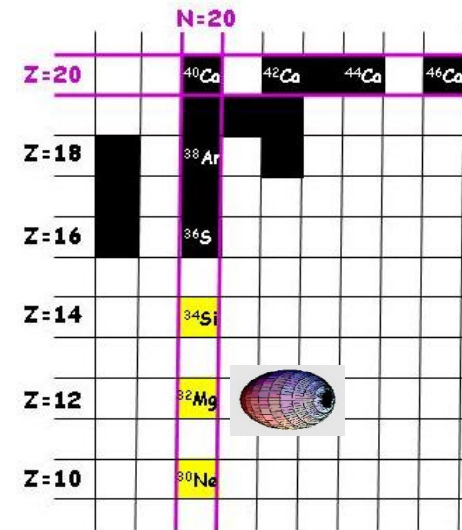
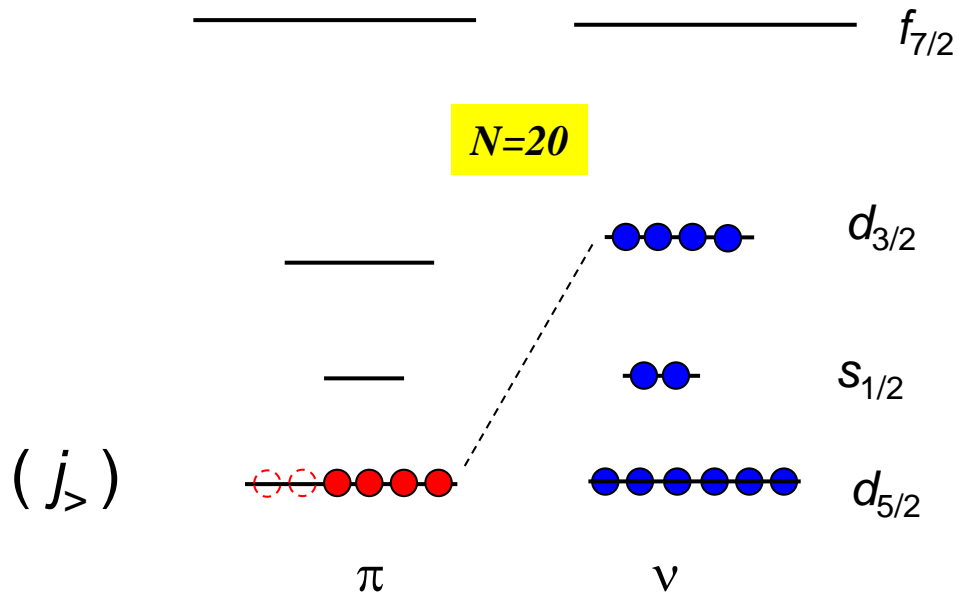


Monopole-interaction of the tensor force

Experimental evidence of the magic number

N=20

$^{32}_{12}Mg_{20}$

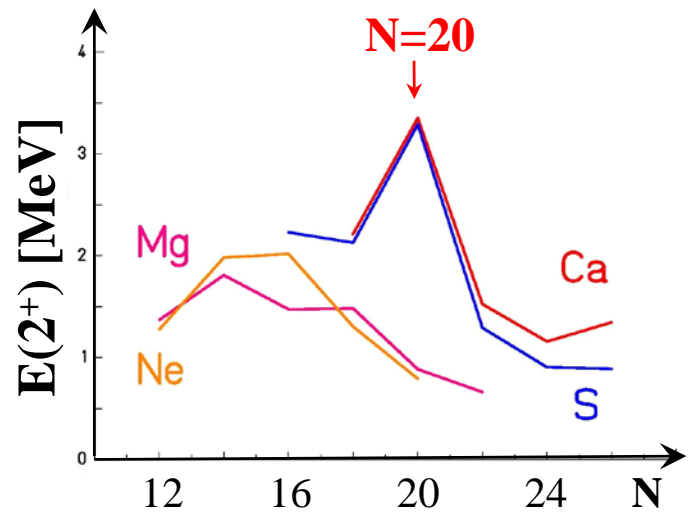
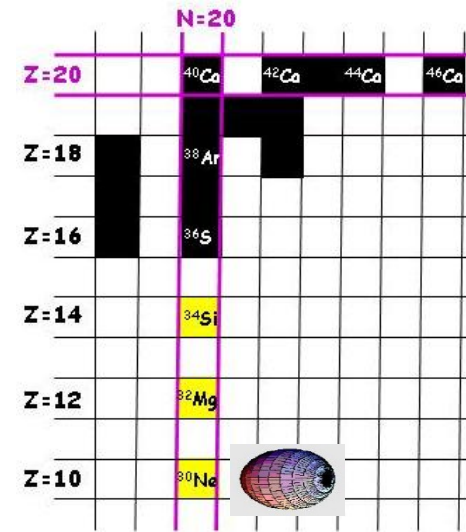
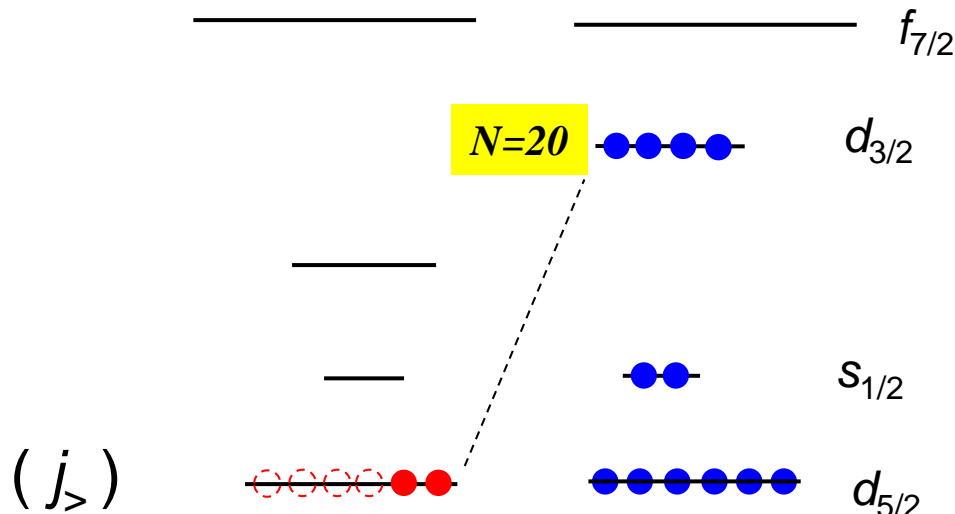


Monopole-interaction of the tensor force

Experimental evidence of the magic number

N=20

$^{30}_{10} Ne_{20}$

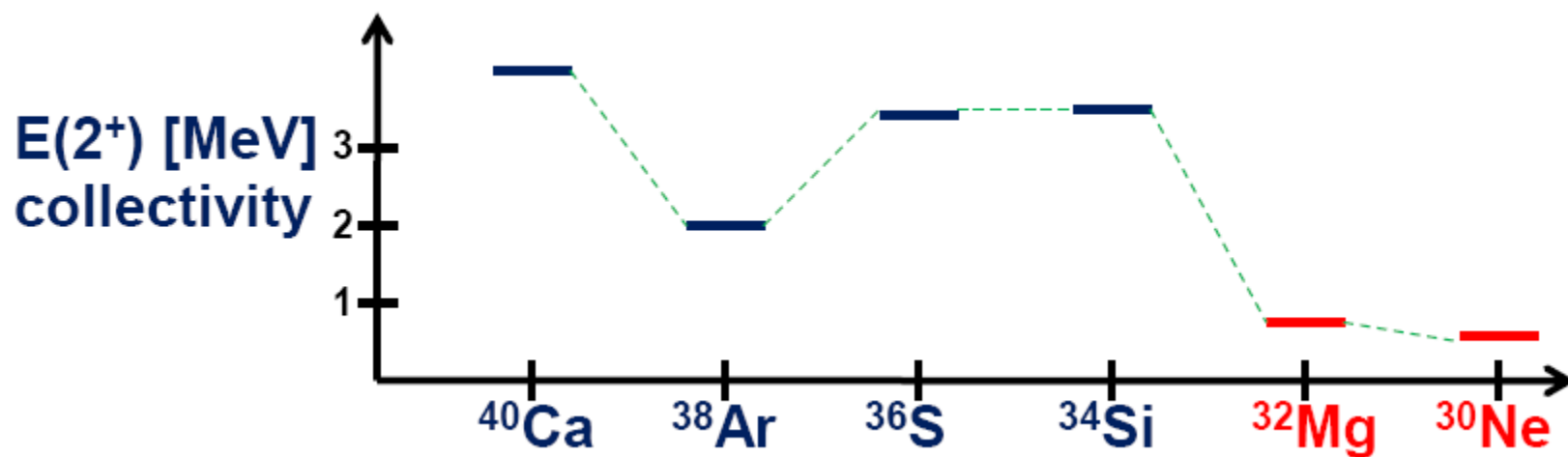
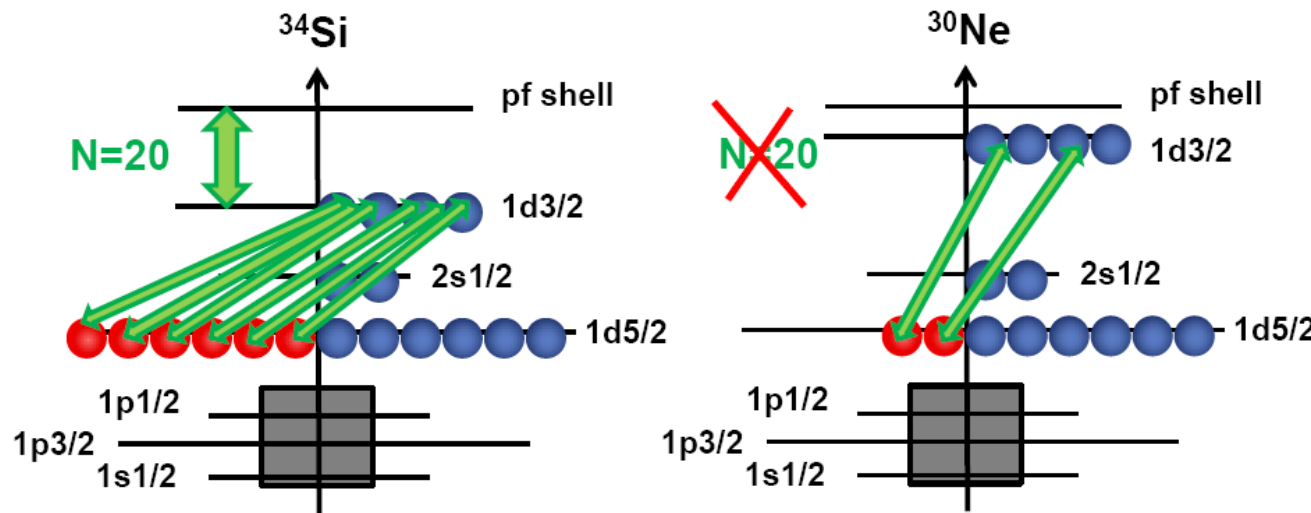


Nuclear shell structure

Experimental evidence of the magic number

$N=20$

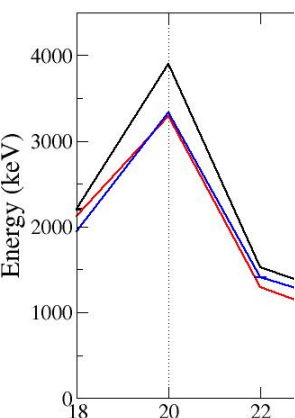
The shell structure is strongly influenced by the attractive p-n force between $J_>$ and $J_<$ orbitals ($\pi d_{5/2}$ and $\nu d_{3/2}$).



Nuclear shell structure

Experimental evidence of the magic number

$N=28$

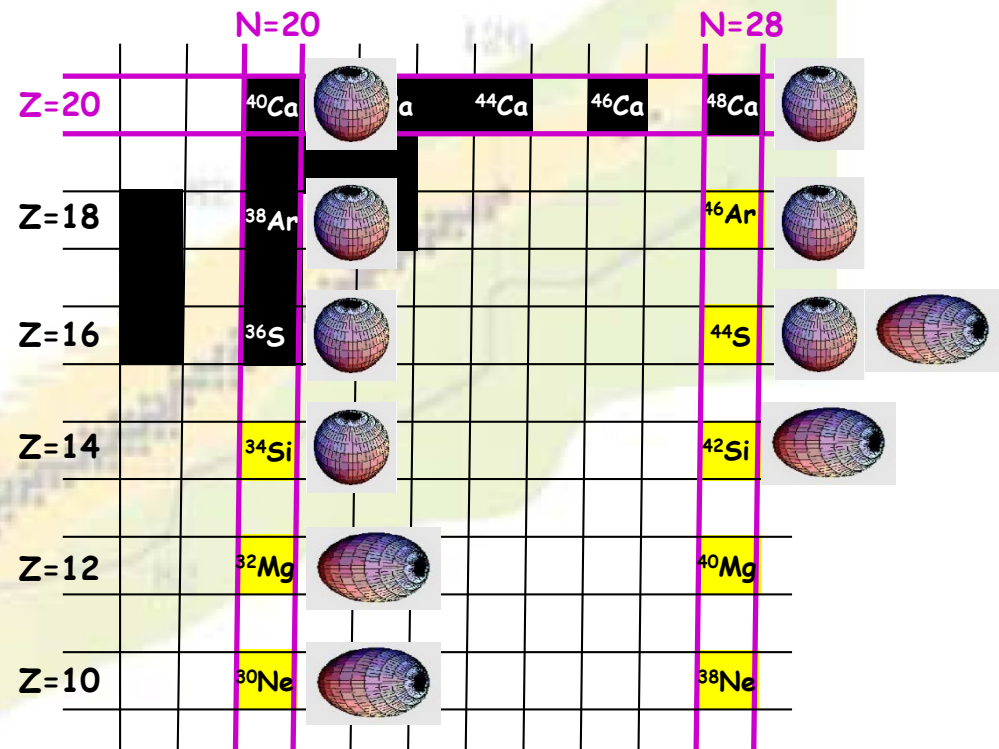


spherical

↑
↓
deformed



S
Si



Evidence of the nuclear shell model:
high energies of the 2_1^+ state
for nuclei with magic number

Nuclear field theory:

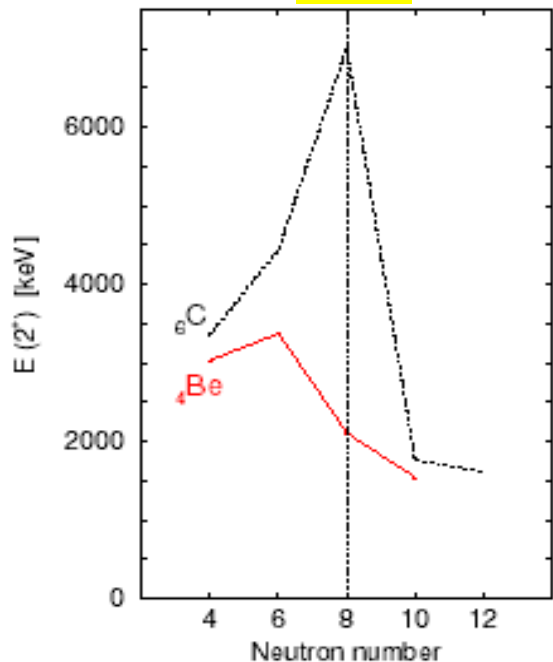
Nuclear many-particle problem will be solved relativistically with the consequence: attractive scalar field (S-V)
repulsive vector field (S+V)

Relativistic quasi-particle random phase approximation

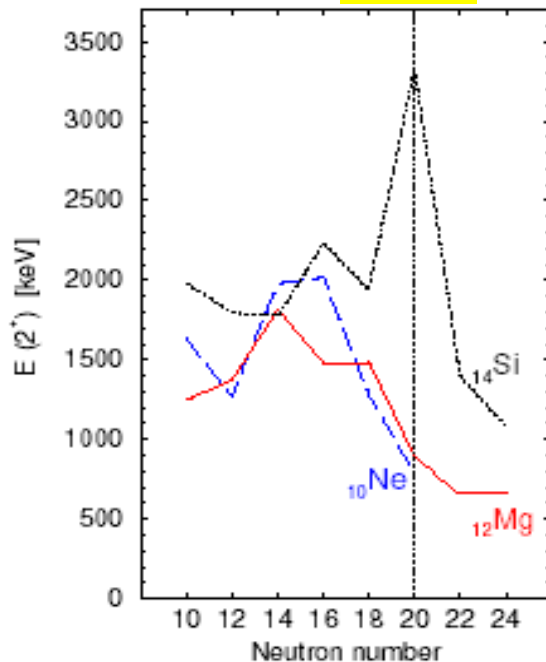
Nuclear shell structure

Large similarity between three numbers of the HO-shell model

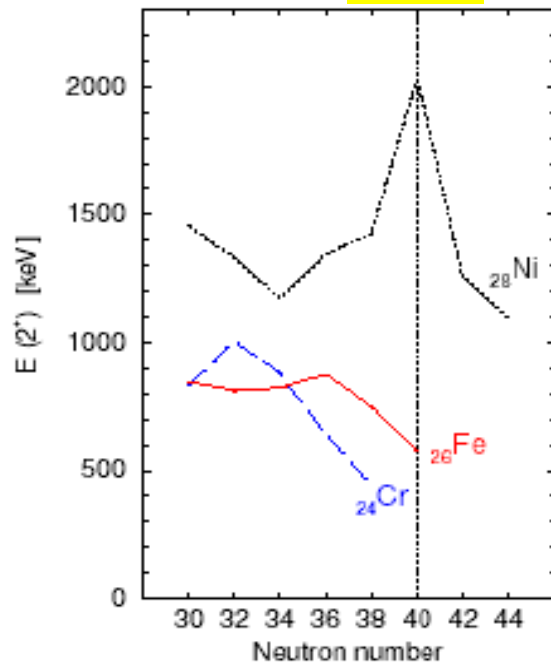
$N=8$



$N=20$



$N=40$



Same mechanism :

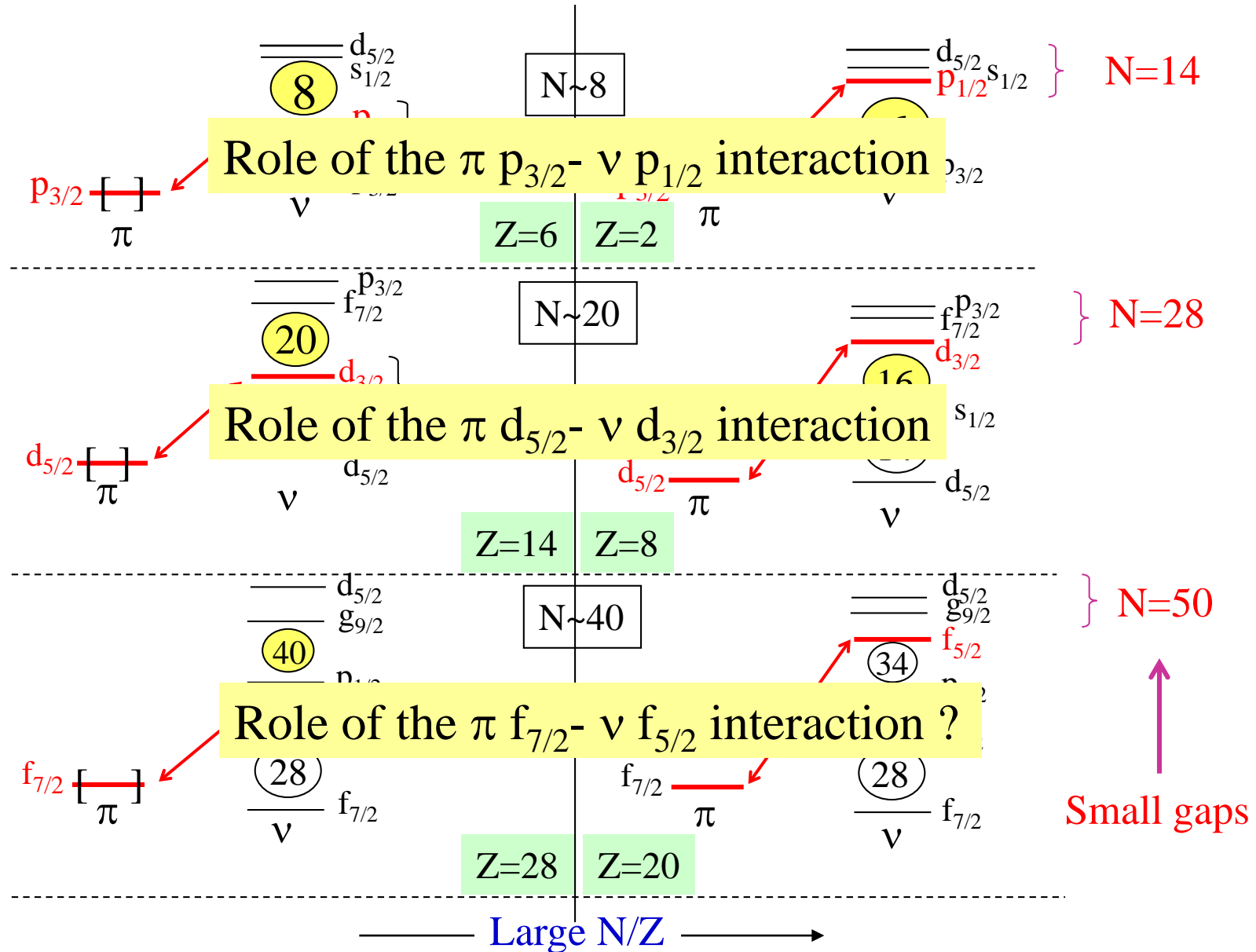
- small 2^+ energies for $N=8$, 20 and 40
- Inversion between normal and intruder states for $N=40$
- Search for a (super)deformed 0^+_2 state in ^{68}Ni
- Proof the extreme deformation of ^{64}Cr

O. S. , MG Porquet PPNP (2008)

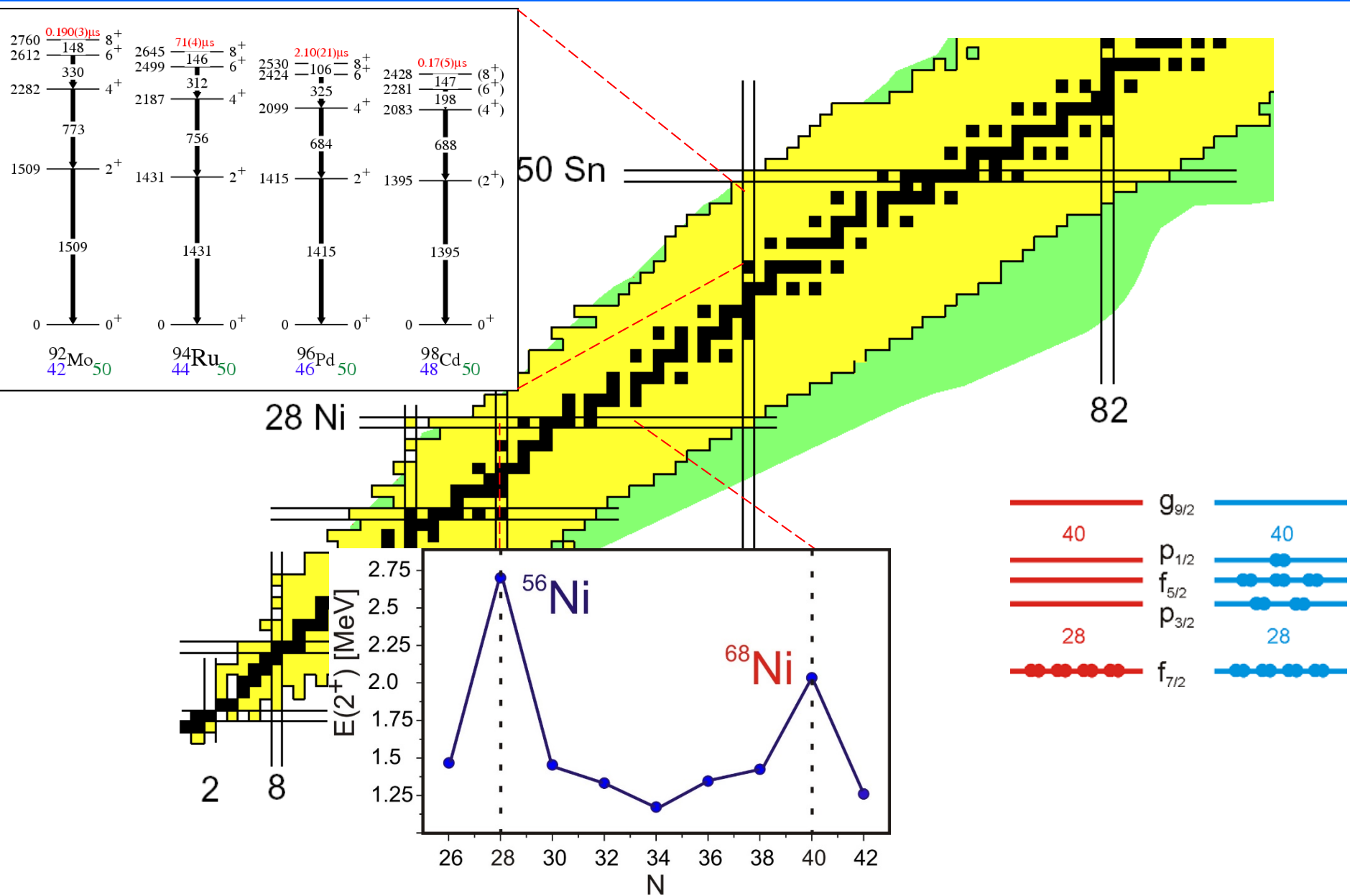
Nuclear shell structure

development of the HO-shell closure

SPIN-FLIP $\Delta\ell=0$ INTERACTION



Nuclear shell structure

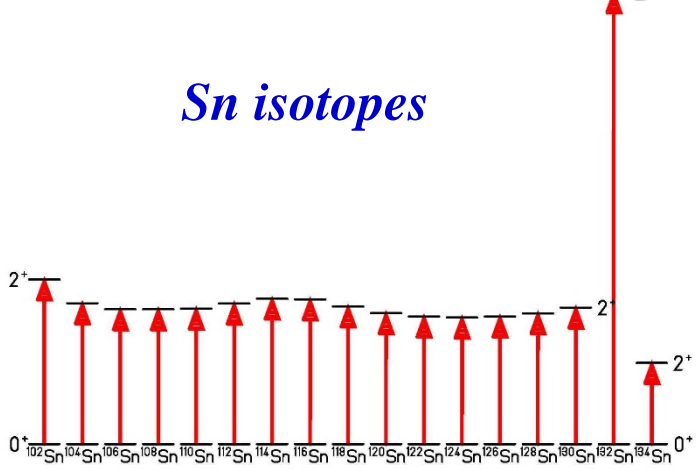




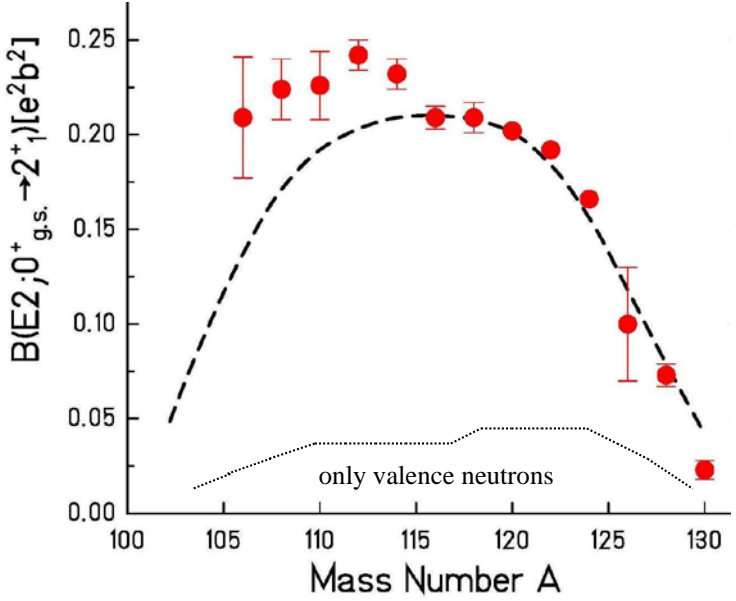
Signatures near closed shells

Sn100 0.94± 0+	Sn101 3± EC	Sn102 4.5± 0+	Sn103 7± EC	Sn104 20.3± 0+	Sn105 31± EC	Sn106 1.90± 0+ (5/2+)	Sn107 10.50± 0+ (5/2+)	Sn108 18.0± 0+ (5/2+)	Sn109 411± 0+ (5/2+)	Sn110 35.5± 7/2+ 0+	Sn111 115.0± 1/2+ 0+	Sn112 115.0± 1/2+ 0+	Sn113 115.0± 1/2+ 0+	Sn114 8.97± 0+ (5/2+)	Sn115 0.65± 0+ (5/2+)	Sn116 0.65± 0+ (5/2+)	Sn117 0.65± 0+ (5/2+)	Sn118 7.69± 0+ (5/2+)	Sn119 7.69± 0+ (5/2+)	Sn120 34.13± 0+ (5/2+)	Sn121 17.00± 1/2+ 0+	Sn122 4.63± 0+ (5/2+)	Sn123 11.12± 1/2+ 0+	Sn124 5.79± 0+ (5/2+)	Sn125 9.64± 1/2+ 0+	Sn126 12.03± 1/2+ 0+	Sn127 11.12± (11/2-) 0+	Sn128 0.61± (5/2+) 0+	Sn129 0.32± (3/2+) 0+	Sn130 3.71± (5/2+) 0+	Sn131 5.63± (5/2+) 0+	Sn132 39.7± (5/2+) 0+	
In99 EC	In100 EC	In101 15.1± (6+)	In102 22.1± (6+)	In103 45.1± (6+)	In104 1.90± EC	In105 5.87± EC	In106 6.2± EC	In107 32.4± EC	In108 58.0± EC	In109 42.1± EC	In110 2.984± EC	In111 4.2± EC	In112 14.97± EC	In113 7.4± EC	In114 71.3± EC	In115 4.418± EC	In116 14.10± EC	In117 43.2± EC	In118 2.4± EC	In119 3.0± EC	In120 23.1± EC	In121 5.99± EC	In122 3.11± EC	In123 2.26± EC	In124 1.69± EC	In125 0.24± EC	In126 1.99± EC	In127 0.24± EC	In128 0.61± EC	In129 0.32± EC	In130 0.25± EC	In131 0.25± EC	In132 0.25± EC
Cd98 0.1± 0+	Cd99 15± (5/2+)	Cd100 49.3± (5/2+)	Cd101 1.36± (5/2+)	Cd102 5.5± EC	Cd103 7.3± EC	Cd104 57.7± EC	Cd105 55.5± EC	Cd106 0+ EC	Cd107 5/2+ EC	Cd108 0+ EC	Cd109 46.5± EC	Cd110 0+ EC	Cd111 1/2+ EC	Cd112 0+ EC	Cd113 7.78± EC	Cd114 53.46± EC	Cd115 0+ EC	Cd116 1/2+ EC	Cd117 2.40± EC	Cd118 50.3± EC	Cd119 3.69± EC	Cd120 50.30± EC	Cd121 13.5± EC	Cd122 5.24± EC	Cd123 2.18± EC	Cd124 1.25± EC	Cd125 0.65± EC	Cd126 0.536± EC	Cd127 0.57± EC	Cd128 0.34± EC	Cd129 0.27± EC	Cd130 0.23± EC	
EC	EC	EC	EC	EC	EC	EC	EC	EC	EC	EC	EC	EC	EC	EC	EC	EC	EC	EC	EC	EC	EC	EC	EC	EC	EC	EC	EC	EC					

Excitation energy



Sn isotopes



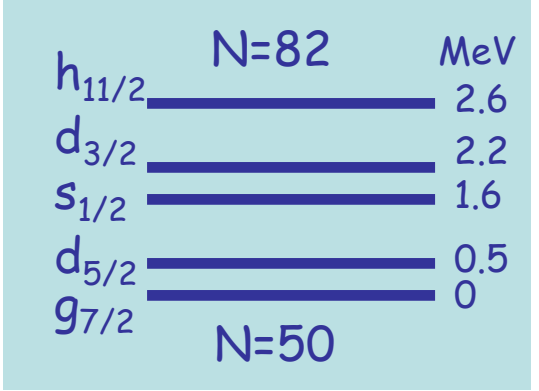
Sn100 0.94+	Sn101 3+	Sn102 4.5+	Sn103 7+	Sn104 20.5+	Sn105 31+	Sn106 115+	Sn107 190	Sn108 10.50	Sn109 18.0	Sn110 411	Sn111 35.5	Sn112 115.0	Sn114 0+	Sn115 1/2+	Sn116 0+	Sn117 1/2+	Sn118 0+	Sn119 1/2+	Sn120 0+	Sn121 17.00	Sn122 0+	Sn123 11.2	Sn124 0+	Sn125 9.64	Sn126 12.5	Sn127 11.2	Sn128 9.87	Sn129 7.55	Sn130 3.72	Sn131 5.63	Sn132 39.7	
ECn	ECn	EC	EC	EC	ECn	EC	EC	EC	EC	EC	EC	EC	EC	EC	EC	EC	EC	EC	EC	EC	EC	EC	EC	EC	EC	EC	EC	EC	EC			
In99	In100 7.8	In101 15.1	In102 22	In103 45	In104 15.0	In105 5.5	In106 6.2	In107 32.4	In108 58.0	In109 4.2	In110 4.8	In111 2.9847	In112 14.97	In113 0.65	In114 0.34	In115 14.53	In116 14.16	In117 14.16	In118 14.16	In119 14.16	In120 3.03	In121 23.1	In122 1.5	In123 5.99	In124 1.5	In125 1.69	In126 1.59	In127 0.61	In128 0.61	In129 0.32	In130 0.25	In131 0.25
	(ECp)	(ECp)	(ECp)	(ECp)	(ECp)	(ECp)	(ECp)	(ECp)	(ECp)	(ECp)	(ECp)	(ECp)	(ECp)	(ECp)	(ECp)	(ECp)	(ECp)	(ECp)	(ECp)	(ECp)	(ECp)	(ECp)	(ECp)	(ECp)	(ECp)	(ECp)	(ECp)	(ECp)	(ECp)	(ECp)		
Cd98 8.1	Cd99 3	Cd100 49.3	Cd101 1.36	Cd102 5.5	Cd103 7.3	Cd104 57.7	Cd105 55.5	Cd106 0+	Cd107 5/2+	Cd108 0+	Cd109 46.5	Cd110 0+	Cd111 1/2+	Cd112 0+	Cd113 7.78+15	Cd114 53.46	Cd115 0+	Cd116 1/2+	Cd117 2.40	Cd118 50.3	Cd119 3.69	Cd120 50.30	Cd121 23.5	Cd122 5.24	Cd123 2.15	Cd124 1.25	Cd125 0.85	Cd126 0.50	Cd127 0.37	Cd128 0.34	Cd129 0.20	Cd130 0.23
	(ECp)	(ECp)	(ECp)	(ECp)	(ECp)	(ECp)	(ECp)	(ECp)	(ECp)	(ECp)	(ECp)	(ECp)	(ECp)	(ECp)	(ECp)	(ECp)	(ECp)	(ECp)	(ECp)	(ECp)	(ECp)	(ECp)	(ECp)	(ECp)	(ECp)	(ECp)	(ECp)	(ECp)	(ECp)	(ECp)	(ECp)	

Cd98
9.2 s
0+
EC

N=50
Z=48

(8+) **2428**
(6+) **2281**
(4+) **2083**

(2+) **1395**



participating neutron-orbitals

(8+) **2128**
(6+) **2002**
(4+) **1864**

(2+) **1325**

Cd130
0.20 s
0+
 β^-n

N=82
Z=48

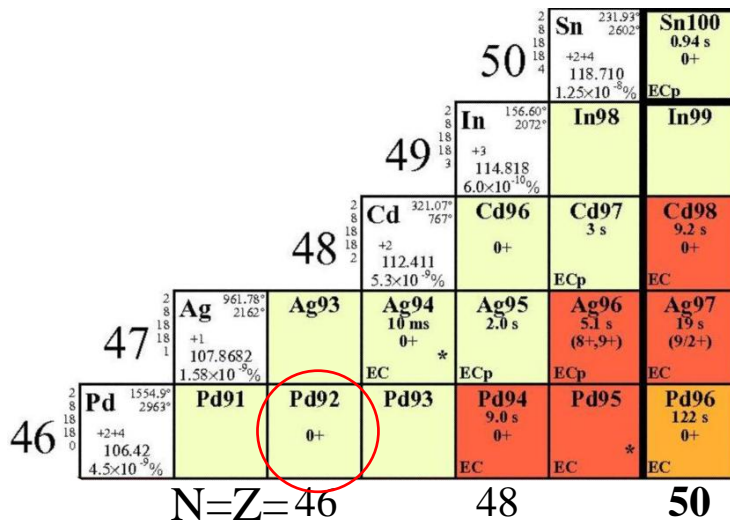
two proton holes in the $g_{9/2}$ orbit

No dramatic shell quenching!

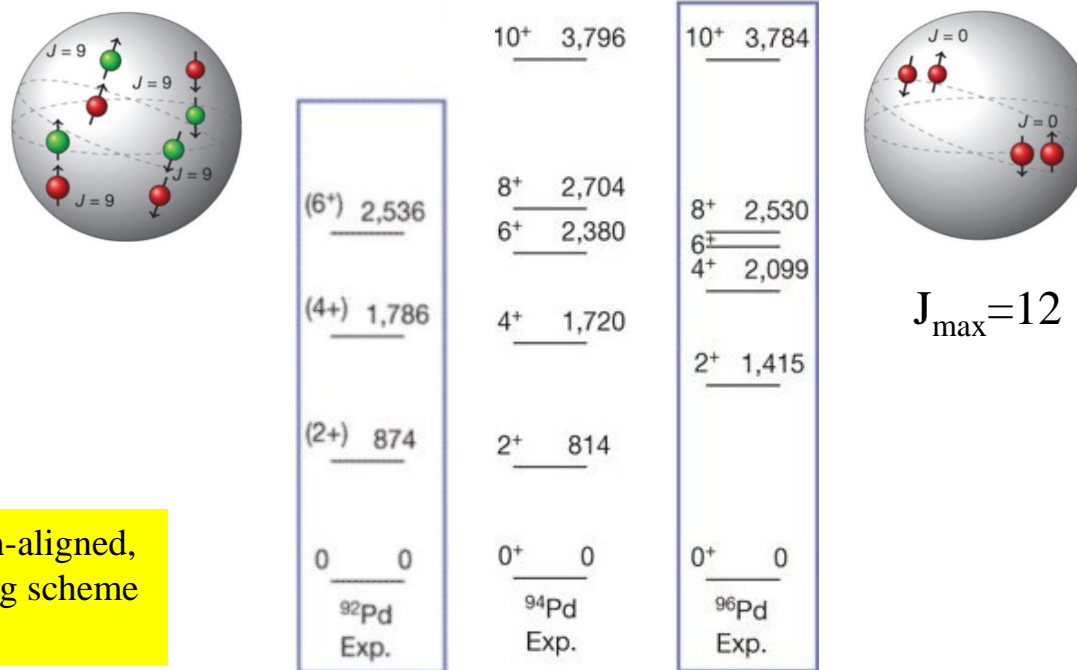
0+ —————

0+ —————

Isoscalar neutron-proton pairing in ^{92}Pd



four proton holes in $g_{9/2}$ orbit

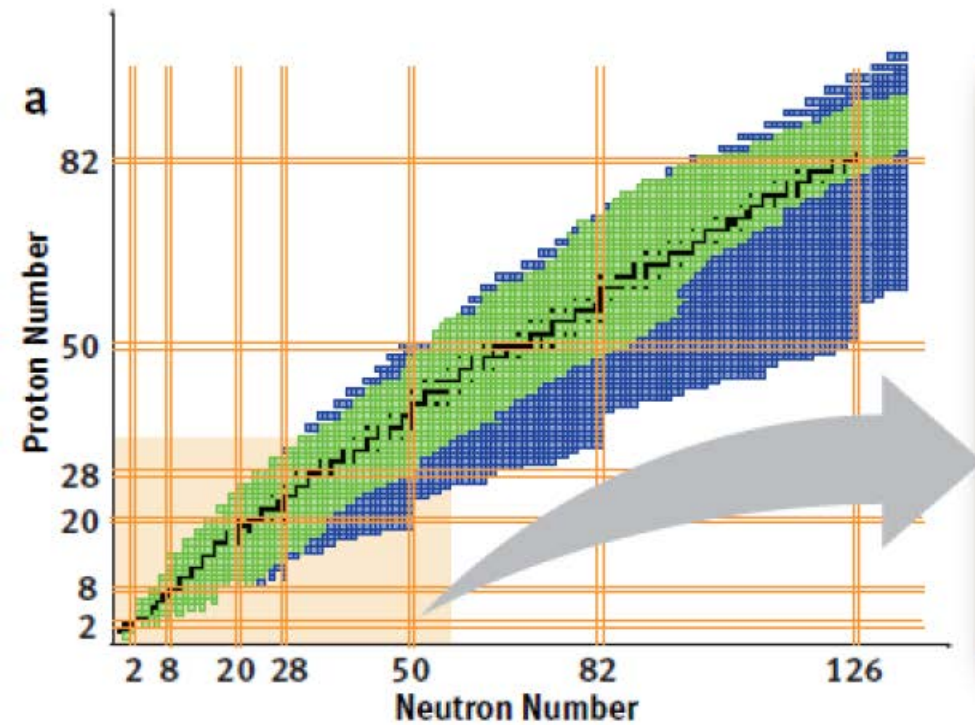


results reveal evidence for a spin-aligned, isoscalar neutron-proton coupling scheme and replaces seniority coupling

B. Cederwall et al., Nature 469 (2011), 68

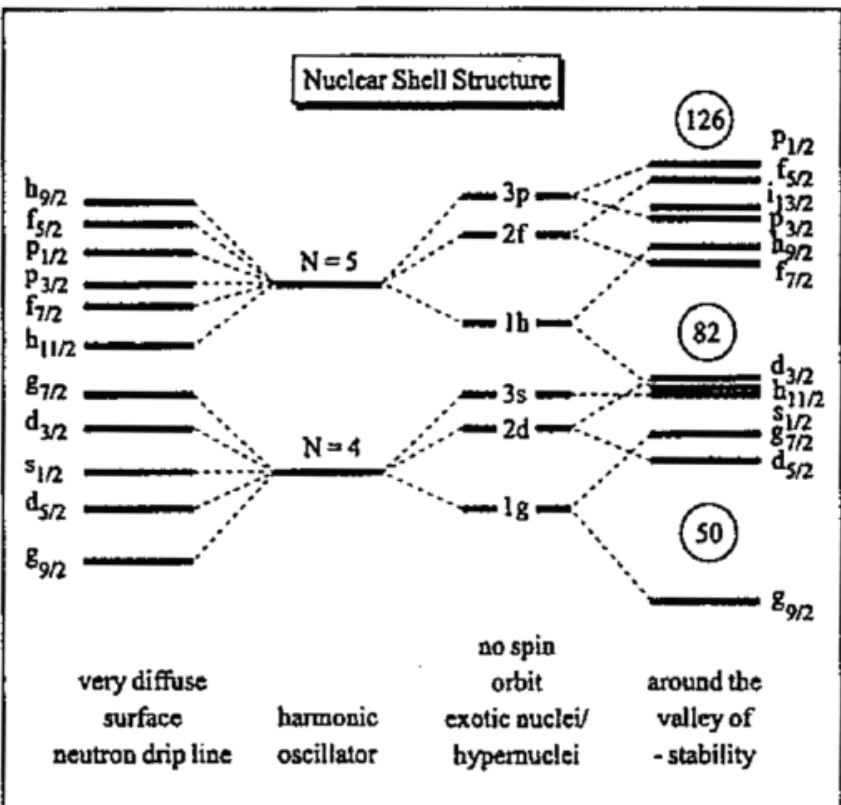
T.S. Brock et al., Phys. Rev. C82 (2010) 061309

New magic numbers

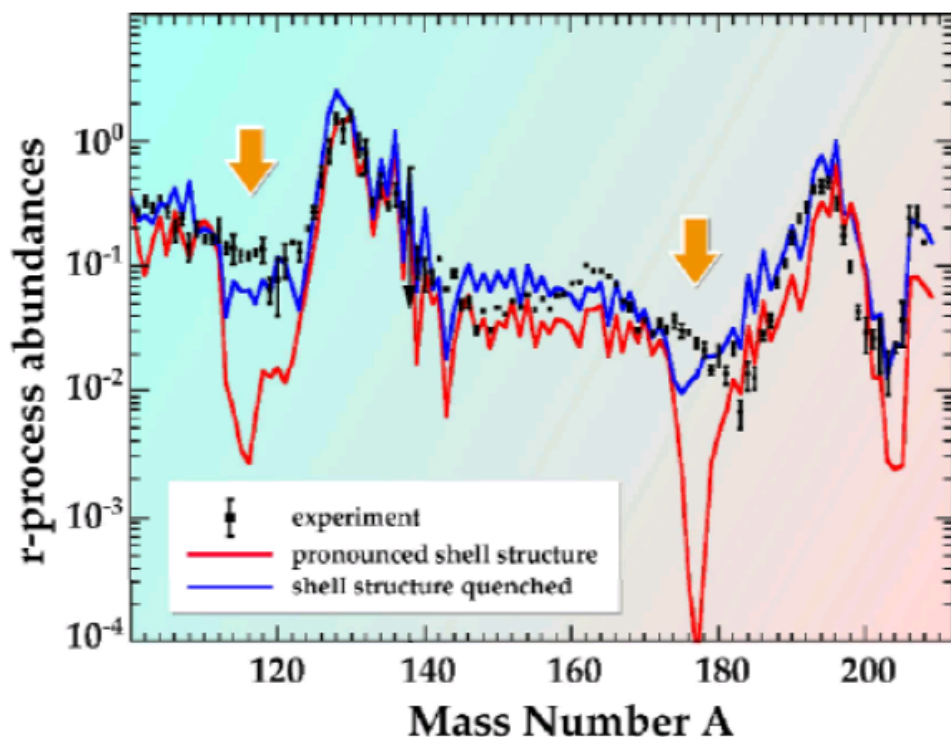




The shell evolution expected for medium-mass and heavy nuclei



The influence to r – process abundances

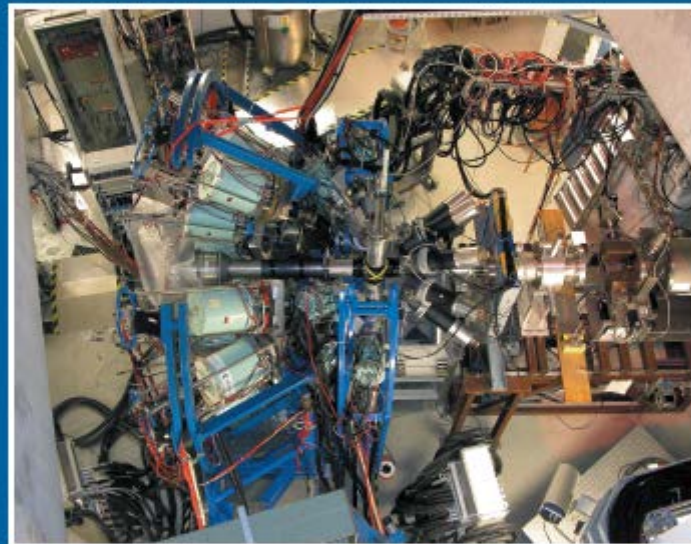


Rare Isotope Beam Capabilities Worldwide



Nuclear Physics News International

Volume 19, Issue 2
April-June 2009



feature article

RISING: Gamma Spectroscopy Far from Stability



Taylor & Francis
Taylor & Francis Group